Dupof DLF-.08798

NDO-10134

NASA-CR 106553

PROGRESS REPORT NGR-01-005-004
PAPERS BY Tuskegee Institute
DR. MICHAEL ERDEY
AND PAPER BY
DR. SANDOR POPOVICS AND
DR. MICHAEL ERDEY

PROGRESS REPORT

on

NASA GRANT NGR 01 - 005 - 004

on

Adapting an AMTRAN Terminal to Graphical Network Theory and to Develop Softwave for adapting AMTRAN to the IBM 1620 Computer

Reported by,

Michael R. A. Erdey, Principal Investigator

Date: August 25, 1969

School of Engineering

Tuskegee Institute

Tuskegee Institute, Alabama, 36088

Introduction

The major objectives of the proposed research were as follows:

I. To build an interface between the IBM 1620 Computer and the NASA A M T R A N terminal (point 3.1 in proposal).

II. Develop and adapt graphical techniques to AMTRAN (points 3.4, 3.5, 3.6 and 3.7 in proposal).

III. Develop software to adapt the rectangular diagram method to the A M T R A N System (point 3.3 in proposal).

IV. Provide programs for on-line interactive mathematical analysis.

The present status of the various sections of the overall program is the following:

I. Present State of the Interface Building

With this extremely critical part of the program, our group had several difficulties:

1. The A M T R A N terminal that we received from Huntsville was adapted to an IBM 1620 Model II Computer and ours is a Model I.

2. There is only one IBM 1620 Model I Computer which has an AMTRAN-terminal and that Computer is at the University of Georgia in Athens, Georgia. In their case, the terminal was built directly for the Model I Computer and, therefore, their case is different from ours.

3. We wanted to use outside consultants, as it turned out, that each of them asked in the range of $6,000.00, which is a much higher figure than we had originally estimated for consultation fees.

Under the given conditions, nothing else remained than to rely entirely on our own resources and to design the whole interface at home, without the aid of outside consultants, but using our own men, (Mr. Stone and Mr. Slatter), in addition to their original duties in the A M T R A N project in after hours as consultants to the interface building, this turned out to be a very rewarding experience for both of them. They learned quite a lot from this experience. Naturally, since neither of them were computer hardware specialists, they had to study first both the IBM 1620 Computer and the A M T R A N-terminal very carefully, before they made their decisions on the interfacing issue. This took quite a lot of time and pushed back the date when the terminal will be in operative condition. The work that has been done in this area and the major decisions that were made are listed below.

The first work on AMTRAN HARDWARE was familiarization with what communication takes place between the AMTRAN terminal and the IBM 1620 computer. This took the form of studying the AMTRAN hardware manual and the IBM 1620 system diagrams. In this study it was clear that certain parts of the interface supplied by IBM and used at NASA would not be duplicated but simulated. Simulation was chosen because fewer modifications to the computer would be required.

After the approach had been determined (simulation) the interface logic and gating was determined. The form of the design was derived using similar C level data communication applications in the IBM 1620 as a guide since technical specifications for the IBM SMS cards were unavailable. Some modifications to the original design were made after limited technical information was obtained from IBM manuals.

While parts were ordered from IBM, work was started on the terminal. The AMTRAN II terminal we are working on is a one-of-a-kind prototype. To provide us with flexibility in moving the terminal from the computer center to the adjacent seminar room and when we move to a new building in November, 1969, plug connectors were substituted for wires connected through screw type terminal strips.

The only other difficulty has been in obtaining parts from electronic distributors. Because of our geographic location, direct communication with distributors for parts supplied and cost is time consuming and costly (long distance phone).

At the present, about 80% of the hardware work is done approximately within 2 weeks, the terminal is expected to be in operative condition.

II. Development and Adaptation of Graphical Techniques to A M T R A N

Due to the delay in the terminal hook-up, software development was also delayed. The efforts were put into working on additional graphical techniques which can be implemented on the A M T R A N-terminal after it is put into operation.

Due to the delay in obtaining the grant, we lost for industry our strong-man in graphical techniques, J. L. Ding. Instead of him, we hired on part-time basis, Dr. Sandor Popovics, former Professor of Civil Engineering Department at Auburn University, and from September on, Professor at the School of Engineering of Northern Arizona University.

Since Dr. Popovic's area of interest is in materials, we tried to find an area in that field, where rectangular diagrams (the major topic of our proposal) can be employed. Since rectangular diagrams are so useful in the analysis and design of electrical networks, we had to find an area in materials science where electrical network analysis can be used. Such an area is, for example, the elastic deformation of solids with the aid of the laminated models.

Laminated models of composite materials can be represented with series-parallel resistive network analogs. The modulus of elasticity of each phase at first sight, can be represented with a fixed resistor. The problem is created by the blending ratios which make the resistors variable. This is the reason why in the enclosed paper on "A Graphical Approach to Determine the Elastic Deformation of Linear N-Phase Composite Solids" the rectangular diagrams don't appear in their direct form. These diagrams were developed from rectangular diagrams, where the slope of the diagonal of a rectangle is equal to the element value, can be seen from the fact, that the slopes of all the lines starting at point O are equal to the modulus of elasticity of the pertinent material. In the second paper entitled "Rectangular Diagram Approach to Determine the Elastic Deformations of Non-Linear N-Phase Composite Solids", rectangular diagrams directly appear in

the constructions, but the blending ratios complicate the diagram constructions again. In a joint paper by Popovics and Erdey, entitled: "Simplified Calculations for E Based on Composite Models for Concrete" rectangular diagrams are entirely eliminated and triangular diagrams are introduced. These diagrams are very excellent for 3-phase composites, and can be used even without the necessity of a graphics terminal, too. The generalization of these diagrams to the 4-phase case is the tetrahedral diagram which will be manageable only with a graphics terminal.

From the three papers, the joint paper by Popovics and Erdey will be submitted for publication in a professional journal, while the other two will be submitted for presentation on a symposium. All three papers, as they are submitted this time are in their preliminary forms. The final forms of these papers, together with the results produced in the meantime, will be included in the final report.

III. Development of Software to Adapt the Rectangular Diagram Method to the AMTRAN System

Due to the delay in the hardware area, only the groundworks were laid down. We have the basic ideas how we will tackle the problems. Details will be presented in the final report.

IV. Providing Programs for On-line Interactive Mathematical Analysis

This part of the program is postponed until the terminal is in an operative condition.

SIMPLIFIED CALCULATIONS FOR E
BASED ON COMPOSITE MODELS FOR CONCRETE

by

Sandor Popovics, Professor
School of Engineering
Northern Arizona University

and

Michael R. A. Erdey, Professor
Electrical Engineering Department
Tuskegee Institute

ACKNOWLEDGEMENT

The authors wish to give thanks to NASA for its kind permission to publish this material resulting from Research Grant NGR 01 - 005 - 004

The establishment of relationships between the properties of hardened concrete and its internal structure is a difficult task because of the multi-face heterogeneous nature of the material. Since, however, this is a fundamental task, attempts have been made to simplify it by using more or less elementary fictitious structures so-called composite models for the calculation of certain properties of the hardened concrete from the properties and amount of the ingredients. Since all these models are based on simplifying assumptions, their applicability for numberical estimation is limited; but, properly selected models provide useful qualitative information concerning this material behavior that cannot be obtained otherwise. This and the simplicity make the model approach attractive for Engineers.

Composite models have been used in concrete technology mainly for the examination of elastic deformations with the assumption that concrete is a two-phase solid. In this paper the two-phase models are obtained from the application of the average concept instead of the usual stress-strain analysis. This is not only a very simple approach but also provides the opportunity to expand the models for three phases. Calculations related to three-phase composites are usually lengthly. It will be shown that this can be simplified by using triangular diagrams, especially when such diagrams are combined with a computer.

Modulus of electricity of two phase composites.

When one blend two materials to form a two phase composite it is expected that the properties of the composite material are between the pertinent properties of the ingredients. It is also reasonable to expect that under certain conditions a property, for instance the deformability, of the composite will be an average of the corresponding properties (deformabilities) of the ingredients or phases. The three simplest average concepts are the arithmetic, harmonic, and geometric averages. The weighed average modulized of elasticity of two phases are defined as follows:

$$E_a = g_1 E_1 = g_2 E_2 \qquad 1)$$

$$E_{11} = \frac{1}{g_1/E_1 + g_2/E_2} = \frac{E_1 E_2}{g_1 E_2 + g_2 E_1} \qquad 2)$$

$$E_g = E_1^{g1} E_2^{g2} \qquad 3)$$

where

E_1 & E_2 = the modulus of elasticity of phase one and phase two, respectively,

E_a E_h & E_g = weighed arithmetic, harmonic, and geometric average, respectively, E_1 & E_2, and

g_1 & g_2 = fractional volume of phase one and phase two, respectively, that is, $g_1 + g_2 = 1$.

It is easy to see that equation one and the mathematical form

of a so-called "laminated model" where the deformations of the two phases in the composite underload are identical. The simplest mechanical form of this model is shown in figure 1-A as parallel-connected springs. Equation two is the mathematical form of the laminated model where the stresses in the two phases are identical. The mechanical model of this formula is shown in figure 1-B as series-connected springs. These models were made popular in concrete technology by Hansen's writings. (1) (2). Equation three does not have a simple spring equivalent, it is a so-called mathematical model. This was proposed by the writer as where for the introduction of the effect of air content on the modulus of elasticity as well as on several other properties of the hardened concrete. (3).

It has been shown through a neat analysis by Paul (4) that equations one and two represent the upper and lower limits, respectively, between which the modulus of elasticity of any two phase solid can be found in those phases where the phases has the same value of Poisson's Ratio. Therefore, it is reasonable to anticipate again that a combination of these two models results in a better fit between calculated and experimental values. The simplest combinations are the arithmetic and harmonic averages of equations one and two as follows:

$$E_A = A_1 E_a + A_2 E_h =$$

$$= A_1 [g_1 E_1 + g_2 2] + \frac{A_2}{g_1/E_1 = g_2/E_2} \qquad 4)$$

$$\frac{1}{E_H} = \frac{A_1}{E_a} + \frac{A_2}{E_h} = \frac{A_1}{g_1E_1 + g_2E_2} + A_2 \left[\frac{g_1}{E_1} + \frac{g_2}{E_2}\right] \qquad 5)$$

where

E_a & E_h= Modulus of electricity calculated equation one and equation two, respectively,

E_A & E_H = weighed arithmetic and harmonic average, respectively, of E_a & E_h , and

A_1 & A_2 = fractional volume of composite represented by equation one and equation two, respectively.

The other symbols are identical with the symbol of equations one through three.

The springs models corresponding to equations four and five are shown in figure 1-C and 1-D. It can be seen that these two models represent a step toward the "composite of composites" concept [5] that is, towards multiphase heterogeneous materials which concrete actually is.

Equation four with A = 0.5 appears suitable for lightweight aggregate concrete, while equation five, which may be called the HIRSCH - DOUGILL model [6] [7], again with A = 0.5 for regular structural concrete. The degree of approximation of equation two and, particularly that of equation one are less satisfactory.

Example One.

To illustrate the considerable differences between various averages, values calculated by equations one through five are compared graphically in figure two for the pace when $E_1 / E_2 = 10$, $E_2 = 1$, and $A_1 = A_2 = 0.5$. If, for instance, $g_1 = 0.4$, the following composite moduli are obtained:

$E_a = 4.6$; $E_h = 1.6$; $E_g = 2.5$; $E_A = 3.1$; and $E_H = 2.4$.

Calculations of blending proportions.

The presented equations provide the modulus of elasticity of composite material when the moduli and the amount of the two phases are known. They can also be transformed to provide the g_1 and g_2 blending proportions when the required E_c modulus of elasticity of the composite material as well as the values of E_1 & E_2 are even. It is sufficient to calculate the g_1 values only because $g_2 = 1 - g_1$. The pertinent formulas are presented below.

From equation one:

$$g_{1a} = \frac{E_c - E_2}{E_1 - E_2} \qquad 6)$$

From equation two: 7)

$$g_{1h} = \frac{E_1 (E_c-E_2)}{E_c (E_1-E_2)} = \frac{E_1}{E_c} g_{1a}$$

From equation three: 8)

$$g_{1g} = \frac{\log (E_c/E_2)}{\log (E_1/E_2)}$$

From equation four: 9)

when A = 0.5:

$$g_{1A} = \frac{(2^{E_c} + E_1-E_2) \pm \sqrt{(2E_c + E_1-E_2)^2 + 8E_1 (E_2-E_c)}}{2 E_c (E_1-E_2)}$$

From equation five: 10)

when A = 0.5:

$$g_{1H} = \frac{E_c (E_1-E_2) - 2E_1E_2 \pm \sqrt{[E_c (E_1-E_2)-2E_1E_2]2 + 8E_cE_1E_2(E_c-E_2)}}{2 E_c (E_1-E_2)}$$

where the symbols are identical with the symbols of equations one through five.

When a $E_c \pm \Delta E$ range is given as the requirement instead of a single E_c value, the range of blending proportions can be calculated again by equations six through ten.

A more practical method for this purpose will be discussed in the next paragraph.

Example Two:

For the case of $E_1 = 10$, and $E_2 = 1$, the g_1 blending proportions needed to provide and E_c composite modulus of 4.0 are as follows;

$g_{1a} = 0.33$; $g_{1h} = 0.83$; $g_{1g} = 0.60$; $g_{1A} = 0.56$; and $g_{1H} = 0.70$.

Three Phase Composites

The application of any of the two phase models on concrete is an obvious over-simplification because even the simplest case, the hardened cement paste, consists of three distinct phases, namely the gel of the hydrated cement, the unhydrated cement particles, and the pores. In many cases the concrete can be considered as a three phase composite, hardened cement paste, mineral aggregate, and pores being the phases. So the three phase composite model represents a better approximation to concrete than the two phase model.

The mathematical forms for three phase models can be obtained easily from equations one through three, for instance, by adding a $g_3 E_3$ term to the left side of equation one. Equations four and five remain unchanged except for the changes in E_a and E_h.

In general there are infinitely many phase proportions for three components that can reduce a given E_c composite modulus. By using equations similar to equations six through ten, upper and lower limits can be calculated for the three phase proportions, or additional conditions can be taken into account. In either way, the calculation becomes considerably longer.

triangular diagrams. A comprehensive description of such diagrams is presented elsewhere. [8] Their application for three phase composites is illustrated in figure three. Each point of the E1, E_2, E_3 triangular area represents a group of g_1, g_2, g_3 proportions for the composite. [These proportions are given in figure three in percentage as the triangular coordinate of the point.] Also, each composition corresponds to a E_a value in this triangle. Due to the linearity of the equation for E_a, point, that is compositioned, having identical E_a values form a family of parallel straight lines in the triangle of figure three. Having constructed this simple parallel line system of selected E_a values by dividing the $E_1 - E_2$, $E_2 - E_3$, and $E_3 - E_1$ distances proportionately according to equation one, the E_a value for every possible combination of the three phases can be read directly from the diagram; pore, inversely, the totality of the possible phase combinations for a given E_a value can be read directly from the diagram.

Similar charts can be constructed for the E_{ah} & E_g values respectively, as shown in figures four and five. The only difference is that the family of parallel straight lines for E_h follows a reciprocal scale, while that for E_g follows a logarithmic scale, as indicated by equations two and three, respectively.

A line representing a constant E_A value for three phases can be obtained with good approximation from the combination of E_a and E_h lines in the triangular diagram of figure three . [6] Two E_a lines greater than the required E_A value should intersect two E_h lines smaller than E_A so that for each useful intersection [i] $E_a + E_h = 2\ E_A$, and [ii] the point of intersection be possibly within the triangle. The four lines form two such useful points of intersection which, in turn, define a straight line. This line represents the constant arithmetic averages of properly selected E_a and E_h values with a good approximation, that is, the line of a constant E_A. This construction is illustrated in figure six for $E_A = 5$, by using the six and seven lines for E_a, and the four and three lines for E_h.

An approximate line for a constant E_H value can be obtained quite similiarly in the reciprocal system of figure four by using suitable $1/E_a$ and $1/E_h$ lines. An illustrative example is given in figure seven for $E_H = 5$ [that is, for $1/E_H = 0.2$] by using the 0.125 and 0.175 lines for $1/E_a$, and the 0.225 and 0.275 lines for $1/E_h$.

By repeating this simple construction, assistant of constant E_A as well as E_H lines are obtained which, incidentally, are not parallel anymore. These systems can be used again directly for the estimation of the E_A of E_H values, and for the determination of the full range of possible phase proportions as has been shown for figures three, four, and five.

Inclusion of additional conditions

One of the advantages of using the presented semi-graphical methods in triangular diagram is that equations six or seven can be used rather than equations nine or ten for the determination of phase proportions with a resulting savings in the calculations. Equally important is that these methods lend themselves conveniently to the inclusion of tolerance limits and additional conditions without any complications in the calculations. This is demonstrated in example three.

Example three.

Assume that the moduli of elasticity of the three phases are: E_1=10m E_2=4, and E_3=1, respectively. Determine all the possible phase proportions for E_A=5 $\pm$ 0.5 with additional conditions that the amount of phase one be not more than sixty percent, and the amount of phase three be within ten and twenty-five percent.

The totality of the phase proportion complying with these requirements are shown in figure eight by the point of the hatched area. The construction of the limits of this area from the condition is indicated in the figure. One can see directly the g_{1A} may vary within twenty-seven and sixty percent limits, g_{2A} within fifteen and sixty-three percent limits, and g_{3A} within ten and twenty-five percent limits.

A comparison of this procedure for three phases to equation nine, which is only for two phases, shows clearly the practical usefulness of the recommended triangular method.

Adoption of Computer with graphical terminals

An additional advantage of the presented triangular methods is that they can be adopted conveniently by a computer that has graphical terminals, such as the AMTRAN method.

Triangular Diagrams and Computer Graphics

The above technique was developed with the aim that it will be implemented on a NASA developed AMTRAN graphics terminal connected to an IBM 1620 Computer. In the case of an AMTRAN terminal all information is entered through a keyboard. Triangular diagrams are equally well adaptable to terminals on which inputs can be entered also with the aid of a light pen.

In case a graphics terminal is employed, the number of phases can be increased to four. In that case the equilateral triangles are replaced by tetrahedrons. This case would be quite cumbersome to handle manually and therefore was left out from this article. On the other hand three dimensional objects and diagrams can be very nicely handled on a graphics terminal. Shifting, rotating and taking cross sections of a three dimensional object can be easily handled on a graphics terminal. This is all that is required for the solution of 4-phase problems with tetrahedral diagrams.

REFERENCES

(1). Hansen, T. C., "Strength, Elasticity, and Creep as Related to the Internal Structure of Concrete", Chemistry of Cement. Proceedings of the Fourth International Symposium. Monograph 43. Vol. II. Washington. 1960. pp. 709-723.

(2) Hansen, T. C. "Thermal and Electrical Conductivity and Modulus of Elasticity of Two-Phase Composite Materials. Influence of Poisson's Ratio and Phase Distribution". Rilem Bulletin, No. 31. Paris. June, 1966. pp. 253-256.

(3) Popovics, S.: "The Model Approach to Two-Phase Composite Solids", to be published by the American Ceramic Society soon.

(4) Paul, B., "Prediction of Elastic Constants of Multiphase Materials" Transactions of the Metallurgical Society of AIME, Vol. 218. February, 1960. pp. 36-41

(5) Bates, A. A., "Composites in Construction", Stanton Walker Lecture Series on the Materials Sciences, Lecture No. 1. Presented at the University of Maryland. November, 1963.

(6) Hirsch, T. J., "Modulus of Elasticity of Concrete Affected by Elastic Modulus of Cement Paste Matrix and Aggregate", ACI Journal, Proc. Vol. 59. March, 1962. pp. 427-451

(7) Dougill, J. W., Discussion of Reference [6], ACI Journal, Proc. Vol. 59, September, 1962. pp. 1363-1365.

(8) Popovics, S., "Theory and Application of Triangular Diagrams", RILEM Bulletin, No. 22. Paris. March, 1964. pp.37-43.

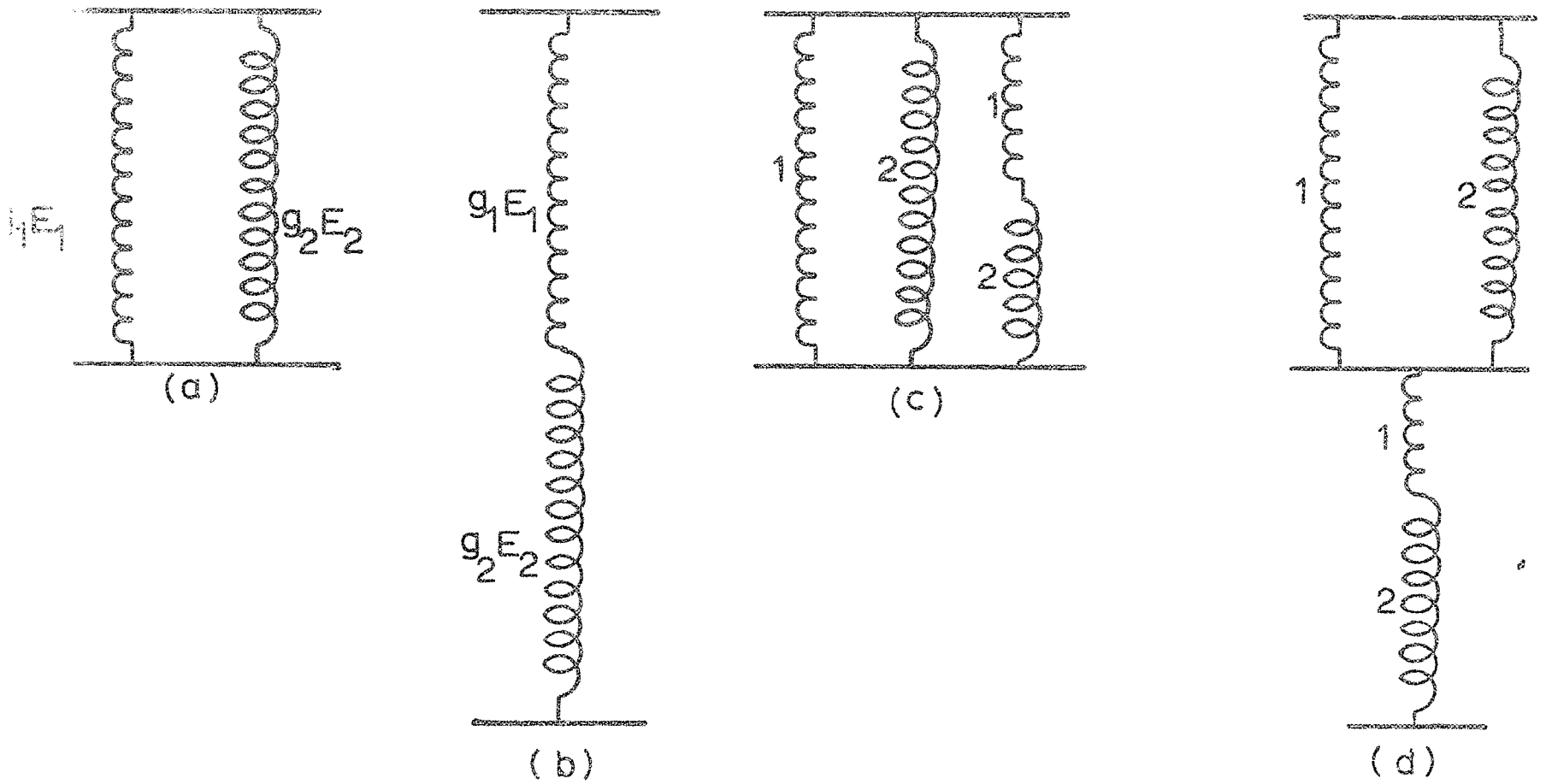

Figure 1. Various spring models for the elastic deformations of two-phase composite solids.

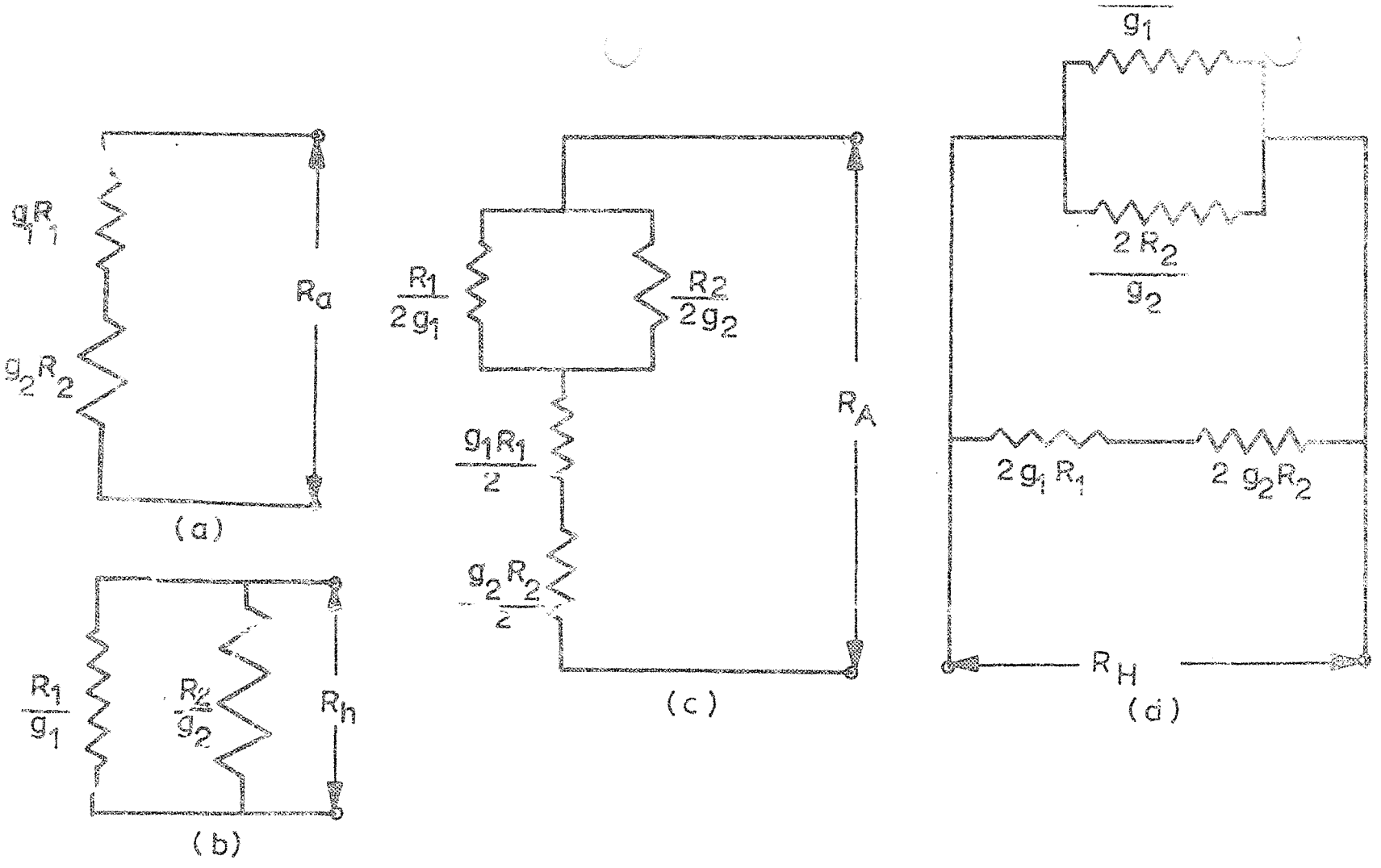

Figure·2 Various electrical network models for the elastic deformations of two-phase composite solids

$$E_a = g_1 E_1 + (1 - g_1) E_2$$

$$E_h = \frac{1}{g_1/E_1 + (1 - g_1)/E_2}$$

$$E_g = E_1^{g_1} E_2^{1-g_1}; \quad \text{(Where)} \quad \frac{E_1}{E_2} = 10$$

$$E_A = \frac{1}{2}(E_a + E_h)$$

$$E_H = \frac{2}{1/E_a + 1/E_h}$$

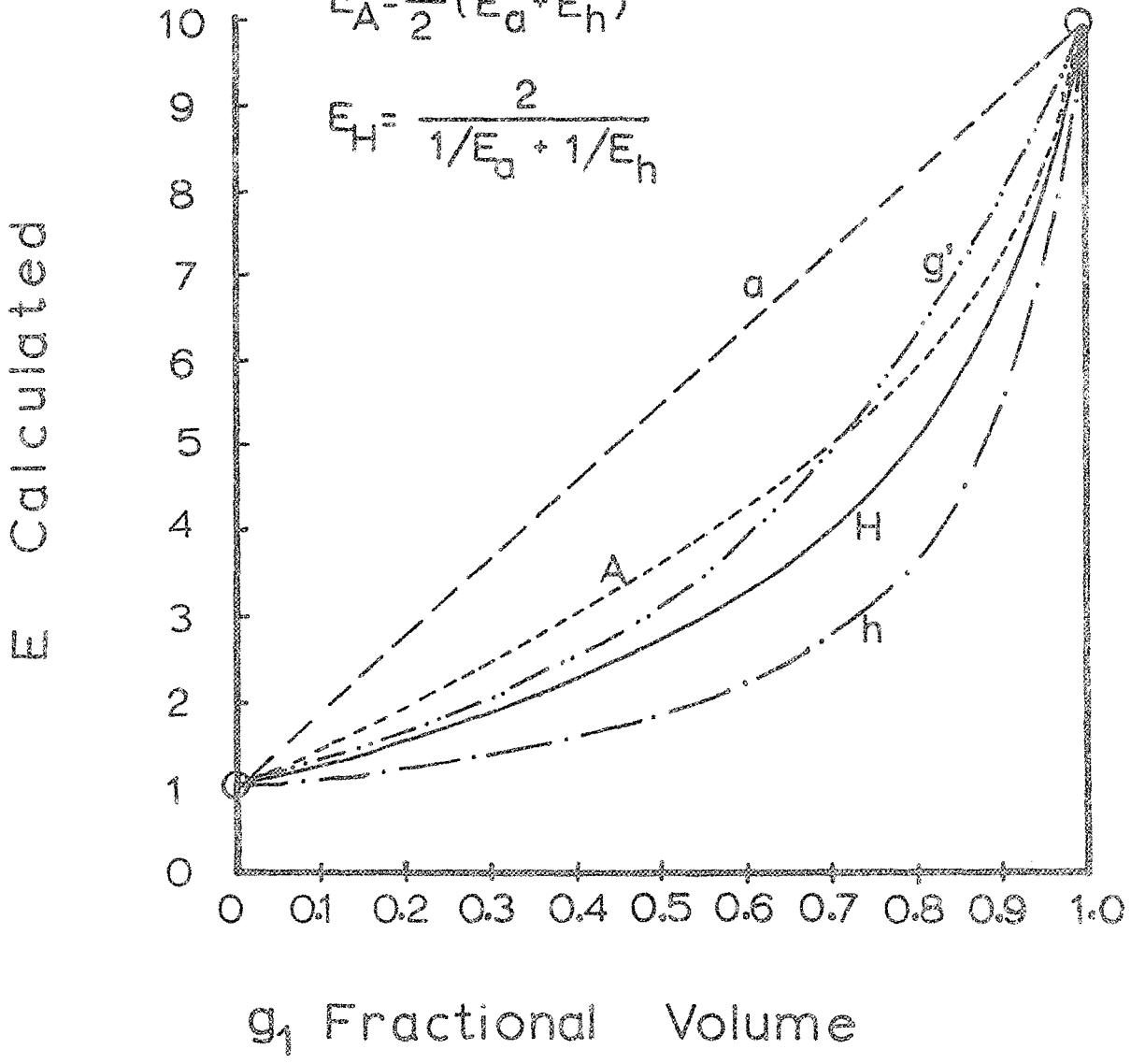

Figure 3. Calculated modulus of elasticity of a two phase composite solid as a function of the phase arrangement and fractional volume of particales.

$$E_a = \sum_{1}^{3} g_i E_i \,; \qquad \sum_{1}^{3} g_i = 1$$

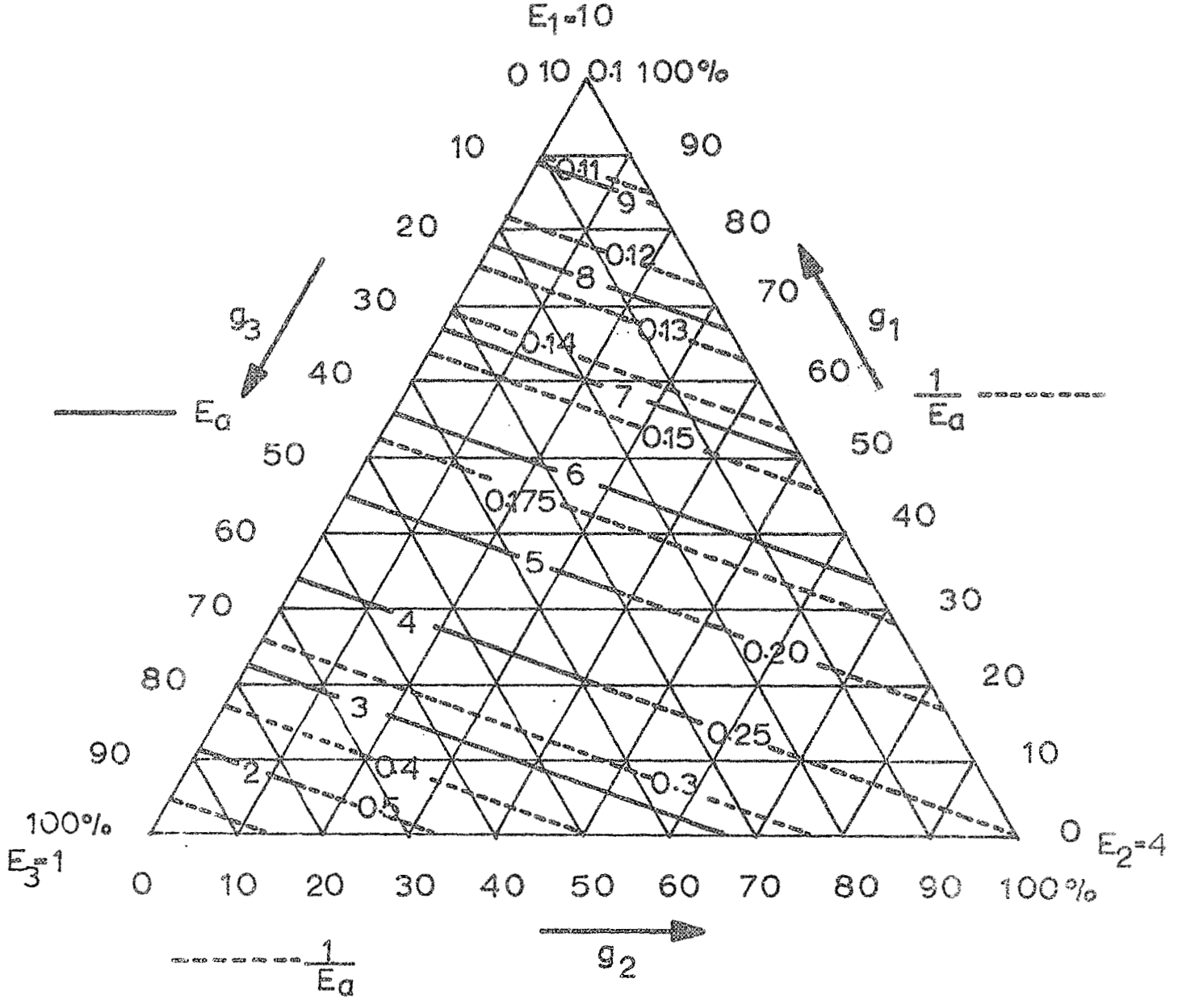

Figure 4

$$\frac{1}{E_h} = \sum_1^3 \frac{g_i}{E_i} \quad ; \qquad \sum_1^3 g_i = 1$$

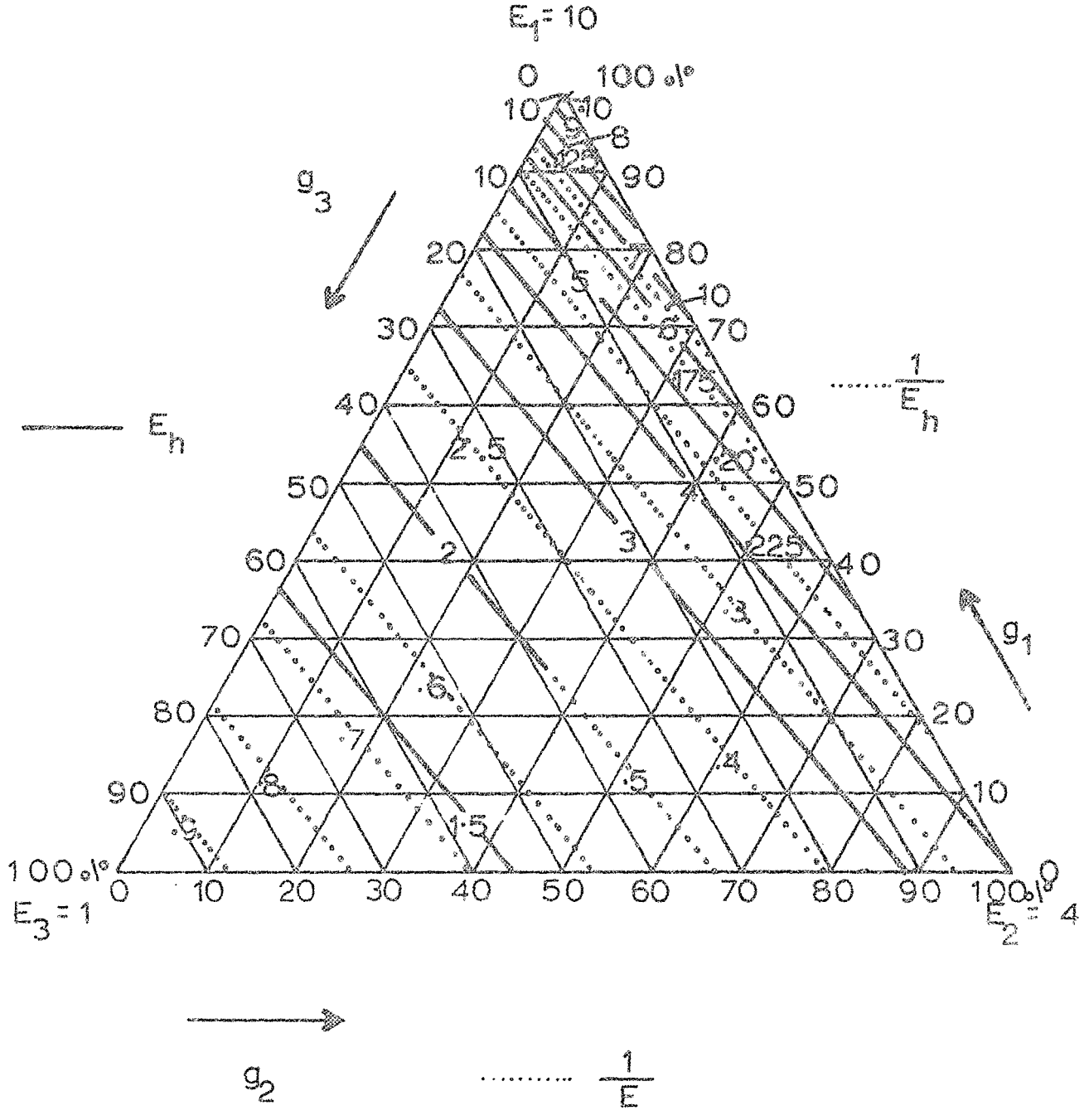

Figure 5

$$E_g = E_1^{g_1} E_2^{g_2} E_3^{g_3} \quad ; \quad \sum_1^3 g_i = 1$$

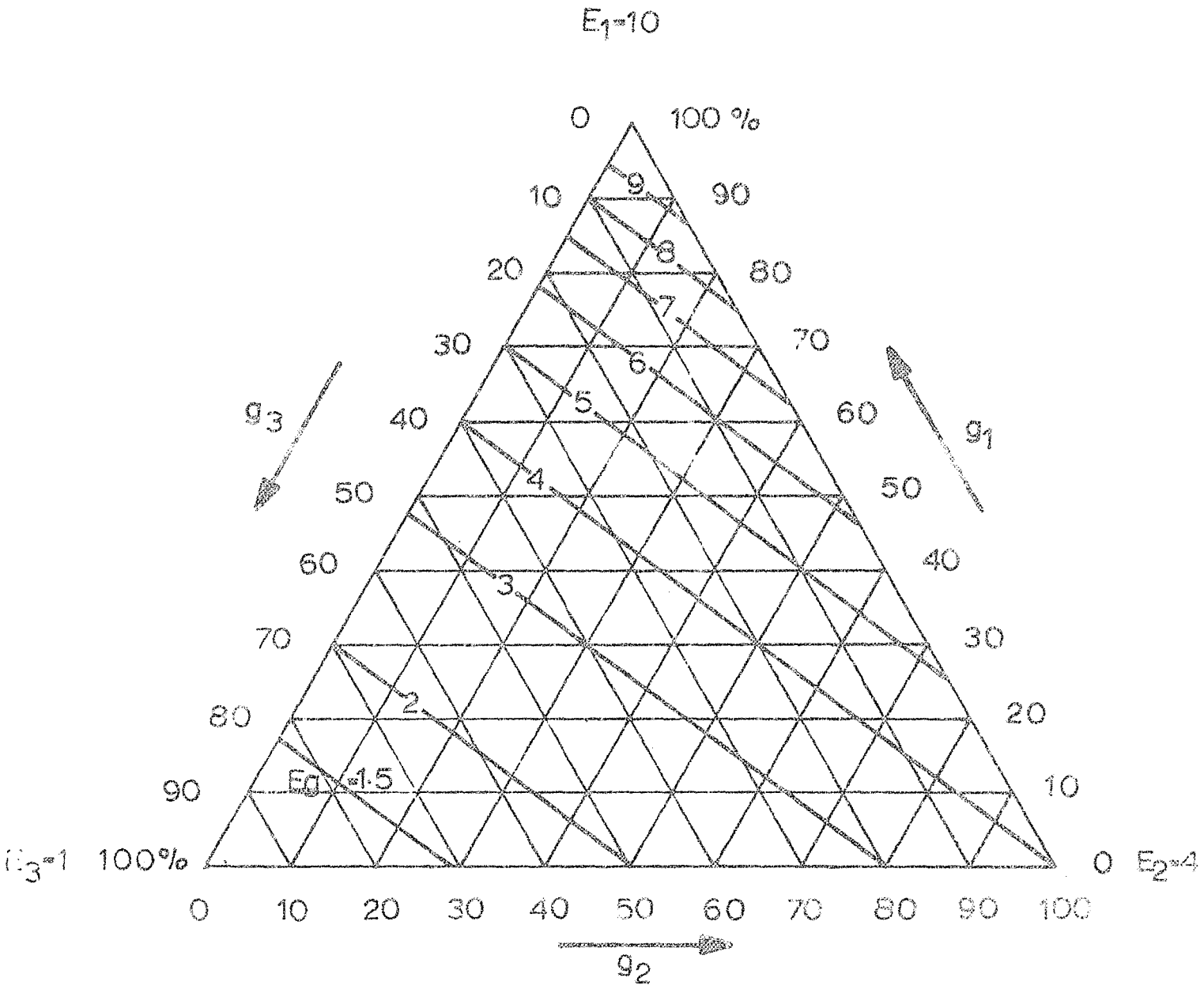

Figure. 6

$E_A = 0.5\ E_a + E_h$

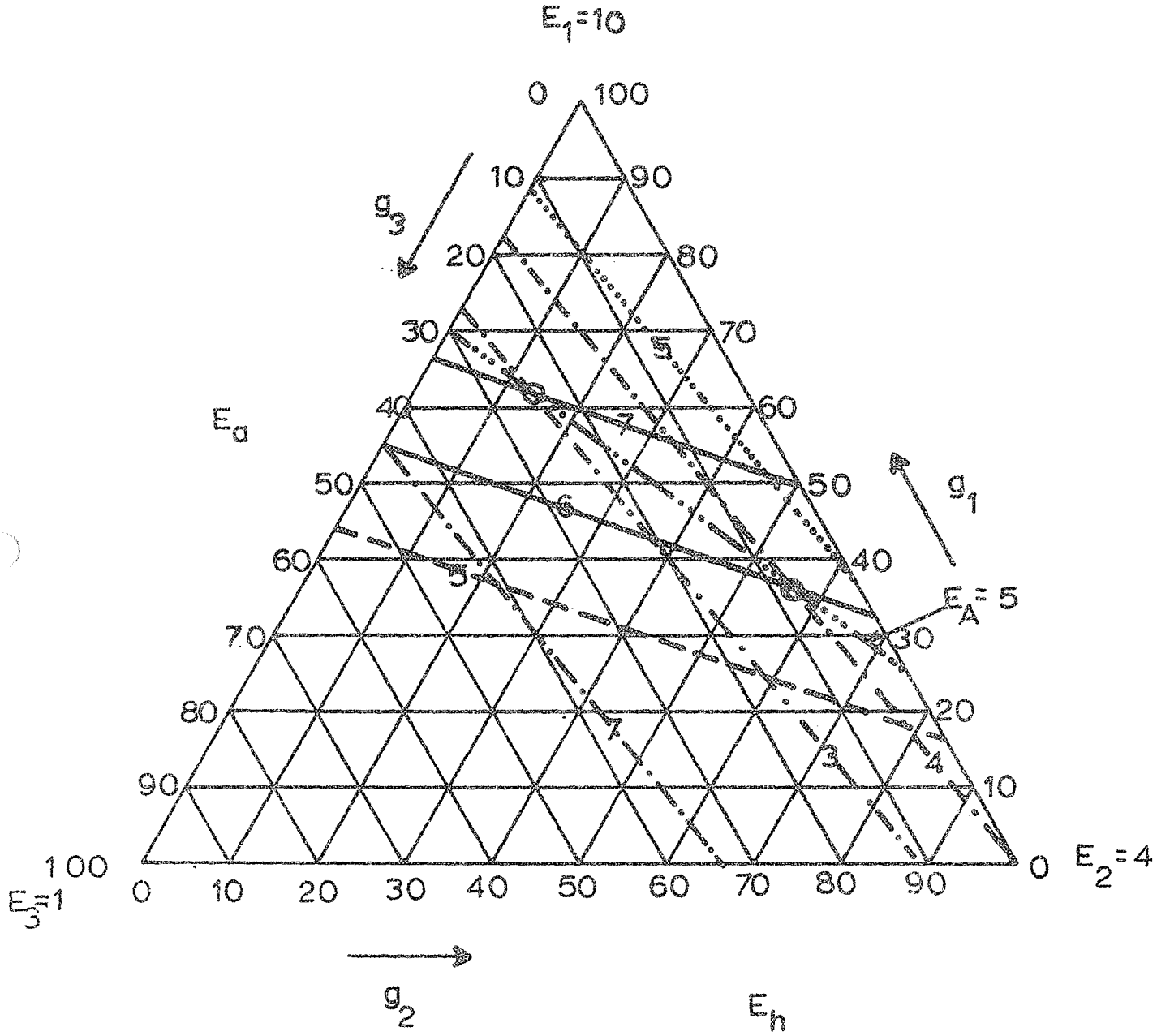

Figure 7

$$\frac{1}{E_H} = \frac{0.5}{E_a} + \frac{0.5}{E_h}$$

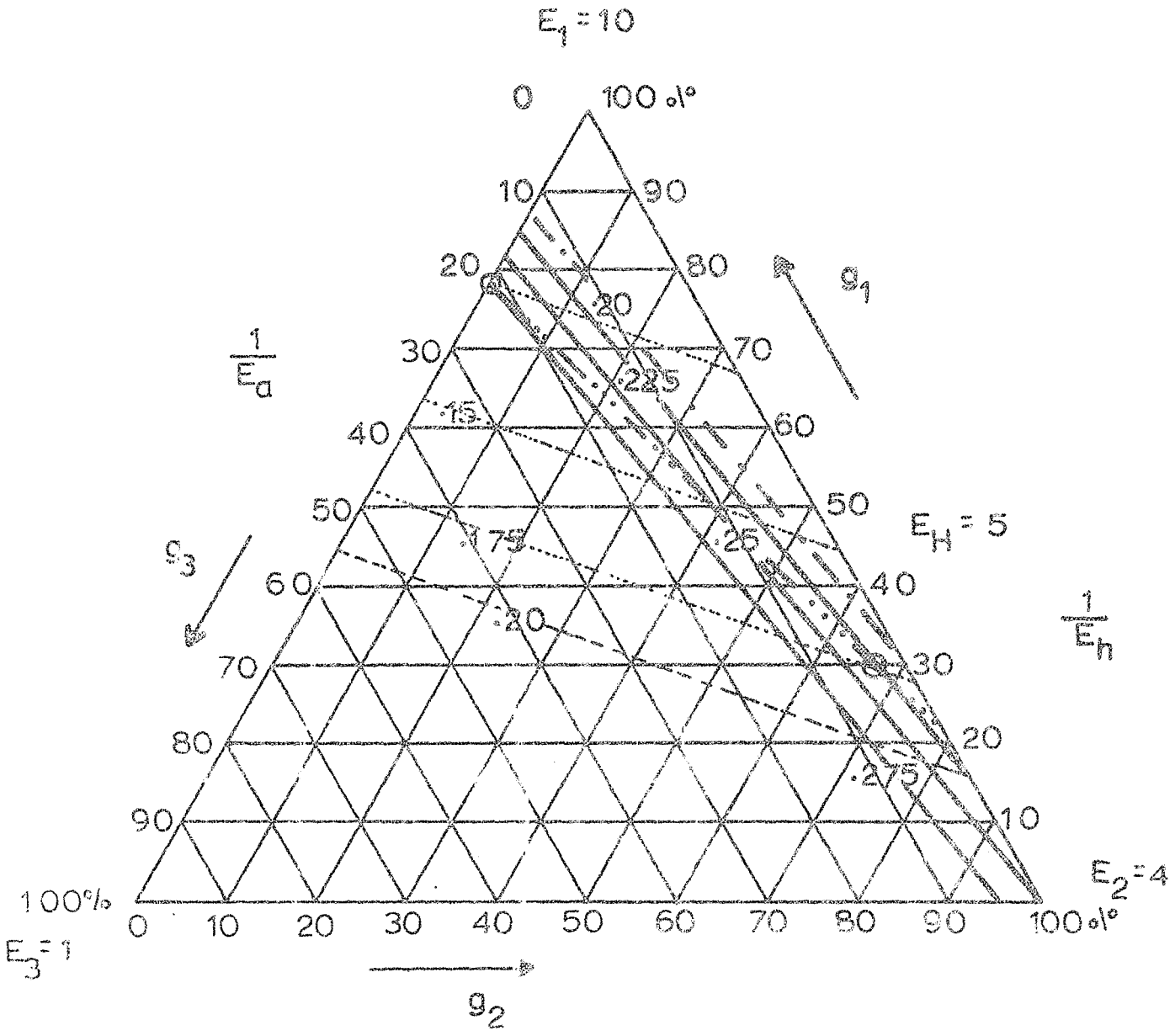

Figure 8

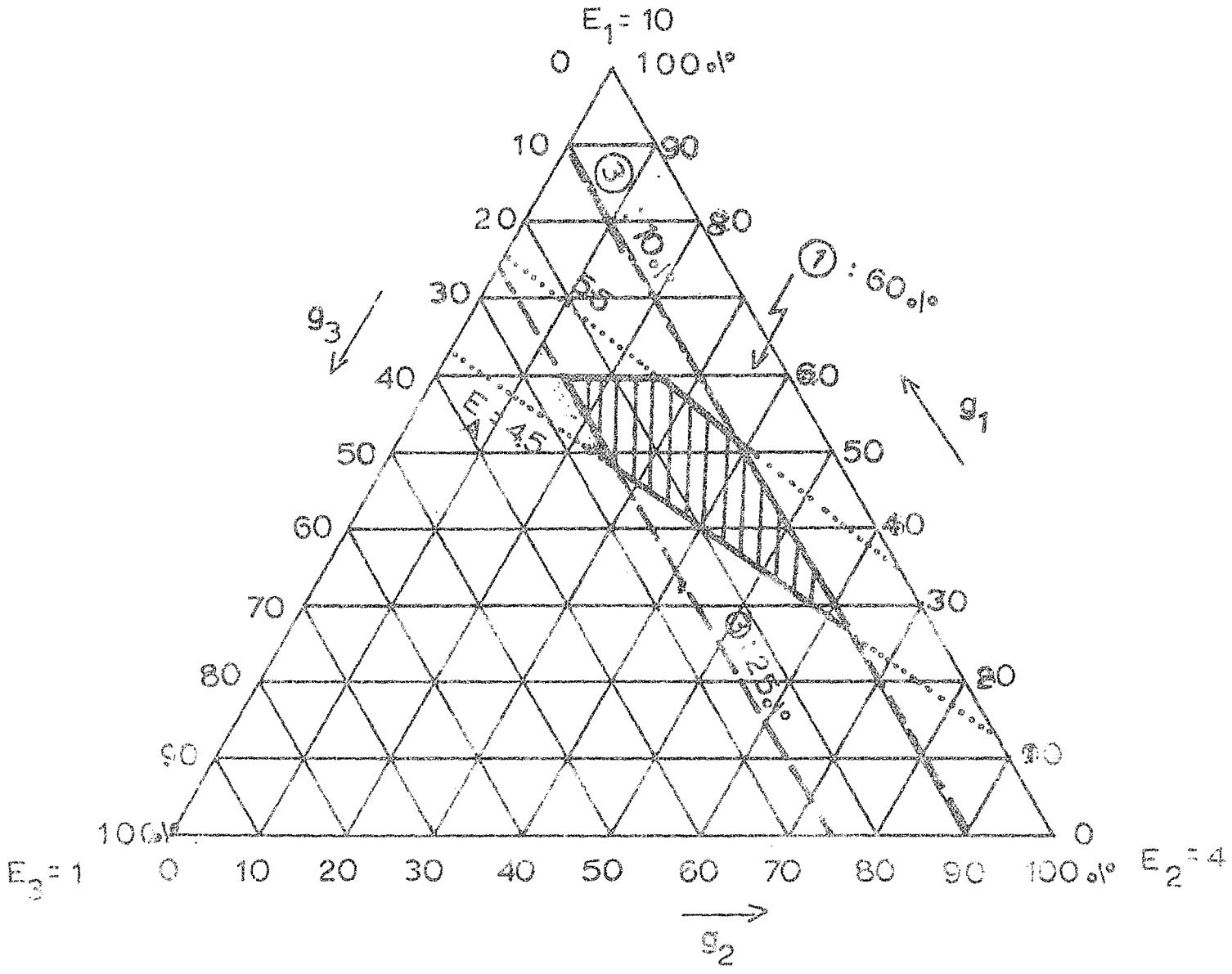
E1 = 10
0
100 o/o
10
90
20
80
30
70
40
60
50
50
60
40
70
30
80
20
90
10
100 o/o
0
E3 = 1
0 10 20 30 40 50 60 70 80 90 100 o/o
E2 = 4
g3
g1
g2
(1) : 60 o/o
(2) : 20 o/o
(3) : 20 o/o
E = 4.5

Figure : 9

RECTANGULAR DIAGRAM APPROACH TO DETERMINE THE ELASTIC DEFORMATIONS OF NON-LINEAR N-PHASE COMPOSITE SOLIDS

BY
Michael R. A. Erdey, Professor

Electrical Engineering Department
School of Engineering
Tuskegee Institute
Tuskegee Institute, Alabama 36088

ABSTRACT

In this article the author applies the rectangular diagram method, which is a very powerful graphical technique to analyze and design electrical networks, to determine the elastic deformations of non-linear n-phase composite solids.

Throughout this paper, the laminar model of composite solids is used, as this model can be represented with simple series-parallel resistive electrical network analogs. Since resistive networks even in the non-linear cases can be handled easily with rectangular diagrams, rectangular diagrams are representing the laminar models throughout this paper.

The paper deals with both the analysis and the synthesis of non-linear n-phase composite solids.

INTRODUCTION

This author has used rectangular diagrams for the solution of linear (1, 2, 4) and non-linear (3) electrical networks.

In the case of non-linear problems, analytical expressions are becoming more and more unmenagable as the complexity of the problem increases. On the other hand, rectangular diagrams can be easily handled even in the more complex cases. An additional advantage of the technique is that it is easily adaptable to a graphics terminal of a computer, such as the NASA developed AMTRAN-terminal.

The Laminar Models and Their Electrical Network and Rectangular Diagram Representation in the Linear Case

In the accompanying paper on the linear case (5), the laminar model and its electrical equivalent, a series parallel resistive network, was fully discussed and, therefore, we do not go into this issue again.

The basis for the electrical equivalent network is the analogy between Hooke's law and Ohm's law as it can be seen from equations (1) and (2):

$$\sigma' = \varepsilon E \qquad (1)$$

$$V = i R \qquad (2)$$

where

σ' = stress

ε = strain

E = modulus of elasticity

v = voltage

i = current

R = resistance

The v-i characteristic curve of the linear resistor of equation (2) or the $\sigma' - \varepsilon$ characteristic curve of a linearly elastic material is represented by a straight line, like the one in Fig. 1-a. The slope of the characteristic curve is equal or proportional if the unit lengths for v and i are chosen differently, to the resistance in the electrical model and to the Young modulus in the elastic model.

If we drop from the P operational point of Fig. 1-a perpendicular to the two axis, we obtain a rectangle, which is redrawn in Fig. 1-b.

In case of a non-linear elastic materials and non-linear resistors the analog equations (1) and (2) go into the analog equation pair of (3) and (4).

$$\sigma = f(\varepsilon) \qquad (3)$$

$$v = f(i) \qquad (4)$$

In this case, the v-i or $\sigma - \varepsilon$ characteristic curves will not be straight lines any more. An example of a non-linear v-i characteristic curve can be seen in Fig. 2-a. From the P operational point, a rectangle can be completed again which is redrawn in Fig. 2-b.

The value of completing the rectangles from the operational points can be clearly seen from the example given in Fig. 3. In Fig. 3-a, a non-linear resistive network is given, its solution in rectangular diagram form is given in Fig. 3-b.

The horizontal sides of the component rectangles are equal (proportional)to the current through the pertinent resistive element while the vertical sides are equal (proportional) to the voltage across it and the area is equal (proportional) to the power consumed by the element. In linear case the slope of the diagonal of the rectangle would be equal to the element value of the linear resistor. Along horizontal lines, Kirchhoff's node laws are satisfied, while along the vertical lines the Kirchhoff's voltage vo

laws are satisfied. The resultant rectangle is the power rectangle of the driver. This rectangle is contiguously filled with the component rectangles, which expresses conservation of energy in graphical form. The solution techniques in rectangular diagram form are given by the author for both the linear and the non-linear cases elsewhere (1,2,3,4) by the author.

Another important fact is that, the rectangular diagrams follow the pattern of the network diagram (4). Since the laminar models can be represented with series-parallel resistive network analogs, the rectangular diagrams will also be placed in a series-parallel contiguous fashion to each other.

The Non-Linear Analysis Problem

For the linear case, the basic equations with the aid of the laminated model (5) were the following:

$$E_a = g_1E_1 + g_2E_2 + \cdots + g_nE_n \qquad (5)$$

$$\frac{1}{E_a} = \frac{g_1}{E_1} + \frac{g_2}{E_2} + \cdots + \frac{g_n}{E_n} \qquad (6)$$

$$E_A = \frac{E_a + E_b}{2} \qquad (7)$$

$$\frac{2}{E_H} = \frac{1}{E_a} + \frac{1}{E_n} \qquad (8)$$

$$g_1 + g_2 + \cdots + g_n = 1 \qquad (9)$$

Note that equation (5) can be represented with a series of connected resistors while equation (6) can be represented with parallel connected resistors. Equation (8) combines (5) and (6) series by which equation (9) represents the parallel interconnections of (5) and (6).

The non-linear equivalents of equations (5) to (8) are given in equations (10) to (13).

$$f_a(\varepsilon) = g_1 f_1(\varepsilon) + g_2 f_2(\varepsilon) + \cdots + g_n f_n(\varepsilon) \qquad (10)$$

$$f_a^{-1}(\sigma) = g_1 f_1^{-1}(\sigma) + g_2 f_2^{-1}(\sigma) + \cdots + g_n f_n^{-1}(\sigma) \qquad (11)$$

$$f_A(\varepsilon) = \frac{f_a(\varepsilon) + f_b(\varepsilon)}{2} \qquad (12)$$

$$\frac{2}{f_H(\varepsilon)} = \frac{1}{f_a(\varepsilon)} + \frac{1}{f_n(\varepsilon)} \qquad (13)$$

Since the $\sigma-\varepsilon$ curves are defined only for positive values the characteristic curves are defined only in the first quadrant of the coordinate system. If we change the negative ε and σ axis into/a positive one as it can be seen in Fig. 4, we can repeat the same function in all four quadrants. Since in all four quadrants, we are representing the same function, with a I to IV subscript, we can express which quadrant is the characteristic curve constructed as it can be seen on the subscripted f in Fig. 4. If the function has already a subscript, then the subscript is followed by a comma and then by the quadrant subscript. If only the first quadrant characteristic curves will be used like in Fig. 6 and Fig. 7, the quadrant subscript will not be used. The usefulness of this notation will be apparent from the application in Fig. 5.

To understand Fig. 5, the reader should note that $f(\varepsilon)$ and $f^{-1}(\sigma)$ are the same functions only the vantage points from which they are looked at are changed; the first is looked from the ε axis which the second one from the σ axis. Therefore, a multiplication by a $g < 1$ factor will shrink the $f(\varepsilon)$ function with the g proportion towards the ε axis and the $f^{-1}(\sigma)$ function will shrink in g proportion towards the σ axis.

In Fig. 5, the case of a non-linear 2-phase composite material is depicted. To obtain accordingly to equation (10) $\sigma_\alpha = f_\alpha(\varepsilon)$ we have to multiply $f_1(\varepsilon)$ by g_1 and $f_2(\varepsilon)$ by g_2. This had been done in this example for $g_1 = \frac{2}{3}$ and $g_2 = \frac{1}{3}$. Having f_1 in the first quadrant and f_2 in the fourth one, the vertical distance between the $\frac{2}{3} f_{1,I}(\varepsilon)$ and $\frac{1}{3} f_{2,IV}(\varepsilon)$ curves will give to every ε the related

value. In a similar fashion by using the $\frac{2}{3} f^{-1}_{1,I}(\sigma')$ and $\frac{1}{3} f^{-1}_{2,II}(\sigma')$ diagrams the $\varepsilon_2 = f^{-1}_{2A}(\sigma')$ is given by the pertinent horizontal distance between the two characteristic curves for each allowable value of σ'.

Combination of equations (10) and (11) into equations (12) and (13) will be very difficult to see in the form of Fig. 5, but will be easily handleable in the rectangular diagram form of Fig. 6 and Fig. 7. In these figures, all first quadrant characteristic curves were included and, therefore, there was no need for double subscript. Secondly, there was no need to include the notations for the functions and their inverse since the parallel connected single rectangles are related to the inverse function. Therefore, instead of the f symbols, we put the pertinent g blending ratios beside the characteristic curves. For convenience in construction, the 2 factors of equations (12) and (13) were left out. Thus, in Fig. 6 the actual $\sigma_A = f_A(\varepsilon)$ is half of the height of Fig. 6, while in Fig. 7 the actual $\sigma_A = f_A(\varepsilon)$ is double of the given height of the diagram.

Both diagrams are given for a particular σ'-ε pair, but can be extremely useful if they are displayed on the graphics terminal of a computer. From these diagrams, the operator can decide in a conversational mode with the computer which parameters to decrease and which ones to increase and with approximately how much in order to obtain the required results. Let's say that our problem is to obtain to a given maximum σ' in the form of Fig. 6 a required value. Lets assume that the height of Fig. 6 is adjusted to the

required a value but E has to be smaller. We can see by inspection that this can be done in this case by decreasing g_1 and increasing g_2. Let us assume that g_1 is decreased to $\frac{1}{3}$ and g_2 increased to $\frac{2}{3}$ ($g_1 + g_2 = 1$ has to be satisfied). We can see that the width of the right rectangle of the two parallel one decreases to its half while the width of the left rectangle increases to its double. Taking into account just by inspection their relative sizes, this operation has to decrease the overall width. At the same time, from the two series rectangles the height of the bottom one will decrease to its half, while the height of the top one will increase to its double. Just seeing their relative sizes this will give some overall height gain which will be compensated by moving towards the left on the respective characteristic curves at the end, since we have to take into account the decrease in the value of $\mathcal{E}$. Thus, we can be sure at a glance that this operation will result in decreasing $\mathcal{E}$ for the same value of .

With the aid of the rectangular diagrams, the general n-phase case for $n > 2$ cases will be equally simple. In that case, instead of two rectangles, we will have n rectangles side by side and n rectangles above each other and the two group will be put again either series to each other or parallel to each other. For example, in case of four elements, we will have the configurations of Fig. 8 and Fig. 9. Since the g blending ratios will be given along the characteristic curves, the operator will be again in the position to judge which parameters should be changed and by approximately how

much by mere inspection of the diagrams. Thus, the rectangular diagrams will serve us as good notations to make the right decisions in an interactive situation on a graphics terminal of a computer.

Concluding Remarks

A very crude justification of the laminar model can be the argument that in composite materials the particles of the various phases are dispersed in all directions. That is: they can be found in parallel and can be found in series too. Therefore, a combination of series-parallel lamination will be nearer to the truth. The "composite soft" and "composite hard" sub-cases make also sense, since a continuous phase should have more effect on the overall behavior of the material and, therefore, if the elastic modulus of the continuous phase is one of the largest (smallest) values we have a "composite hard" (soft) case since the arithmetic (harmonic) mean is always larger (smaller) than the harmonic (arithmetic) mean. But, the physical justification of the laminated model is given by the large amount of experimental data which gives a nice correlation between the measured data and the calculated values from the laminated model. In the case of non-linear materials, this type of correlations are not available yet. The meaning of "composite soft" and "composite hard" material is also not a clear-cut case in the non-linear domain. The σ-ε characteristic curves can be of such, that in a certain operational region the very same material can be looked upon as a composite soft material relative to the other ones while in another operational region it might behave as a "composite hard" material.

ACKNOWLEDGEMENT

This work was sponsored by NASA Grant NGR 01-005-004. The author wishes to thank them for their kind permission allowing this material to be published.

References

1. M. R. A. Erdey: "Rectangular Diagrams and Their Applications to Network Theorems". Proceedings of the Sixth Midwest Symposium on Circuit Theory, pp. F-1 to F-17, Madison, Wisconsin (1963).

2. M. R. A. Erdey: "The Misrepresented Duality and the Rectangular Diagrams". Proceedings of the IEEE Region III Convention, pp. 9.5.1 - 9.5.10, New Orleans, Louisiana (1968).

3. M. R. A. Erdey: "Iterative Solution of Non-Linear Resistive Networks with the Aid of the Rectangular Diagrams". Proceedings of the Eleventh Midwest Symposium on Circuit Theory, pp. 371-388, Notre Dame, Indiana (1968).

4. M. R. A. Erdey: "Rectangular Diagrams in Graph Theory". Proceedings of the Eleventh Midwest Symposium on Circuit Theory, pp. 441-456, Notre Dame, Indiana (1968).

5. M. R. A. Erdey: "A Graphical Approach to Determine the Elastic Deformations of Linear N-Phase Composite Solids". Accompanying Paper.

6. J. C. Haneen: "Theories of Multi-phase Materials Applied to Concrete, Cement Mortar and Cement Paste". Proceedings of the International Conference on the Structure of Concrete, London, September, 1965.

7. B. Paul: "Prediction of Elastic Constants of Multi-phase Materials". Transactions of the Metallurgical Society of AIME, Vol. 218, pp. 36-41, February, 1960.

8. Popovics, S.: "The Model Approach to Two-phase Composite Solids".

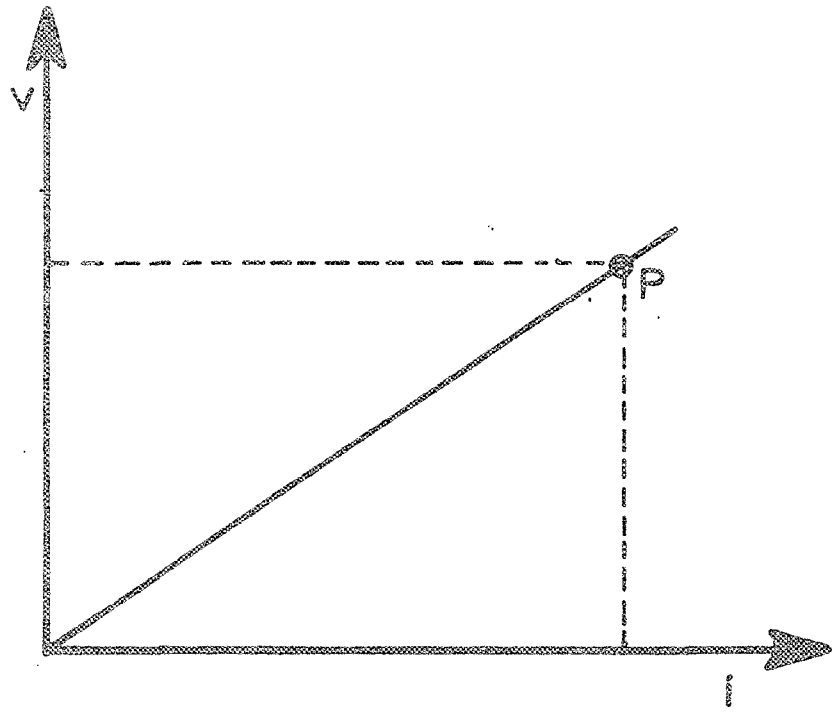

a.

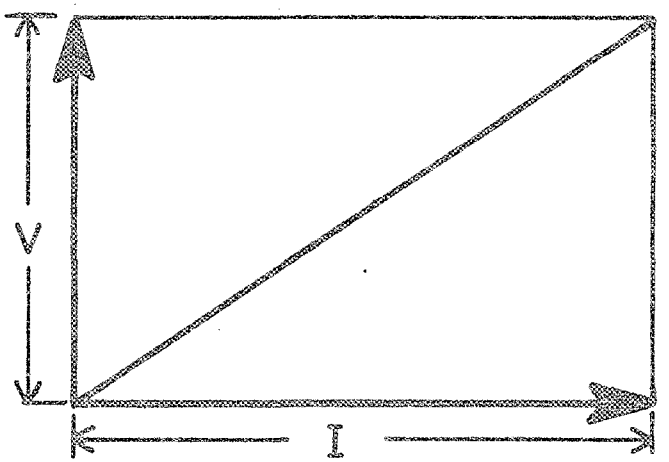

b.

FIG. 1

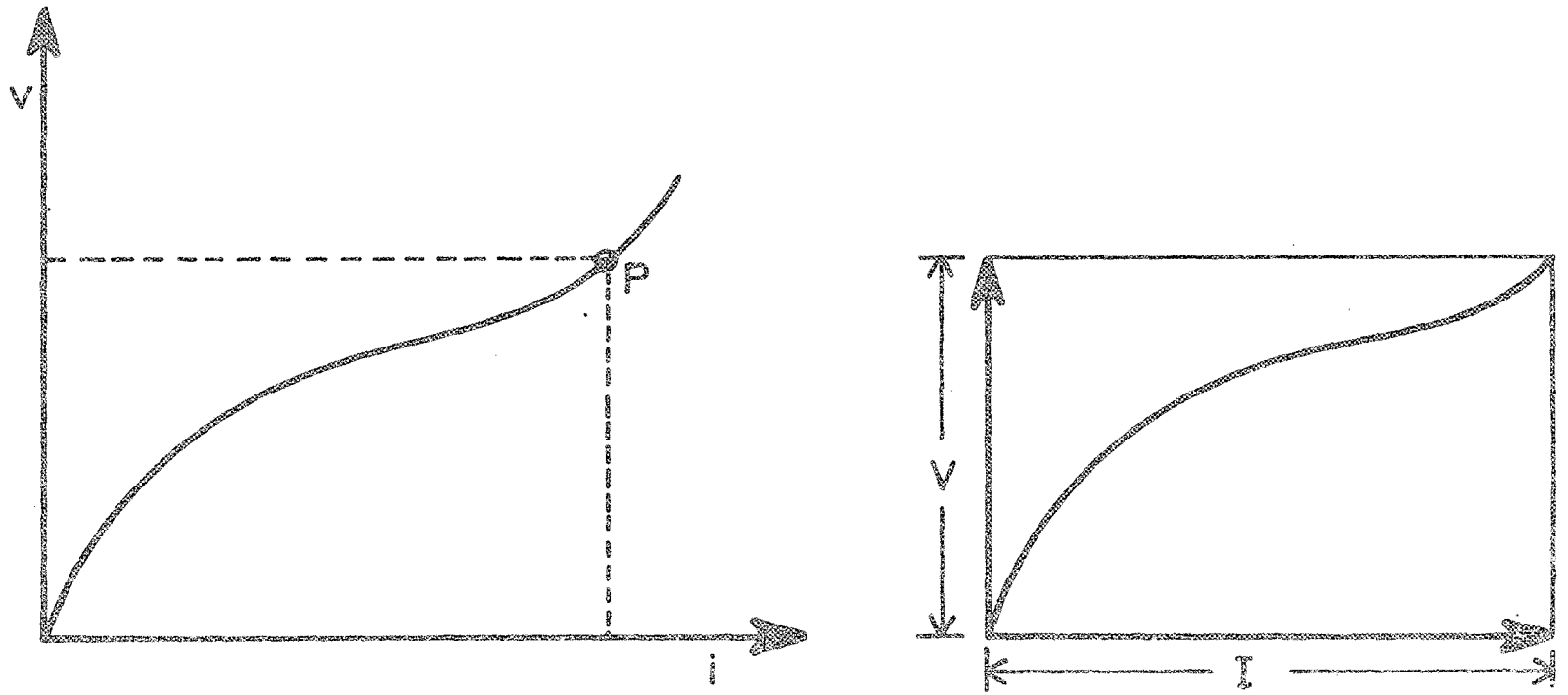

Figure 2

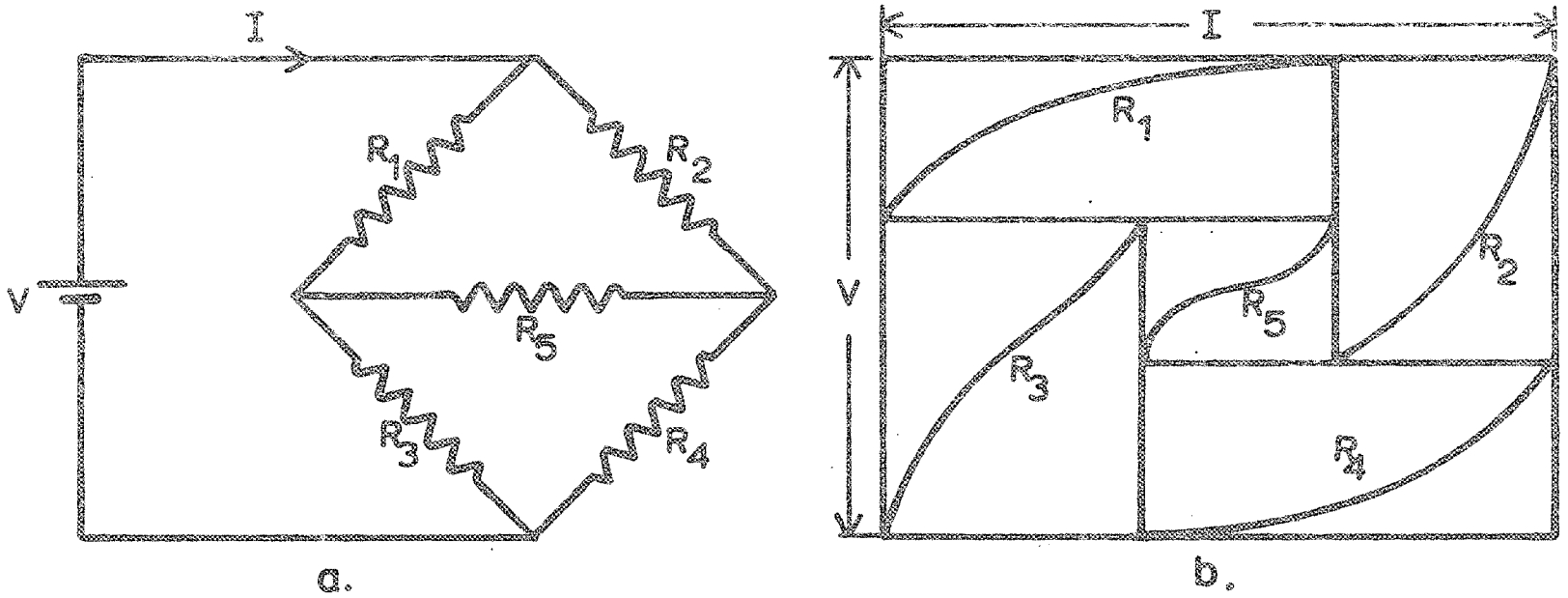

Figure 3

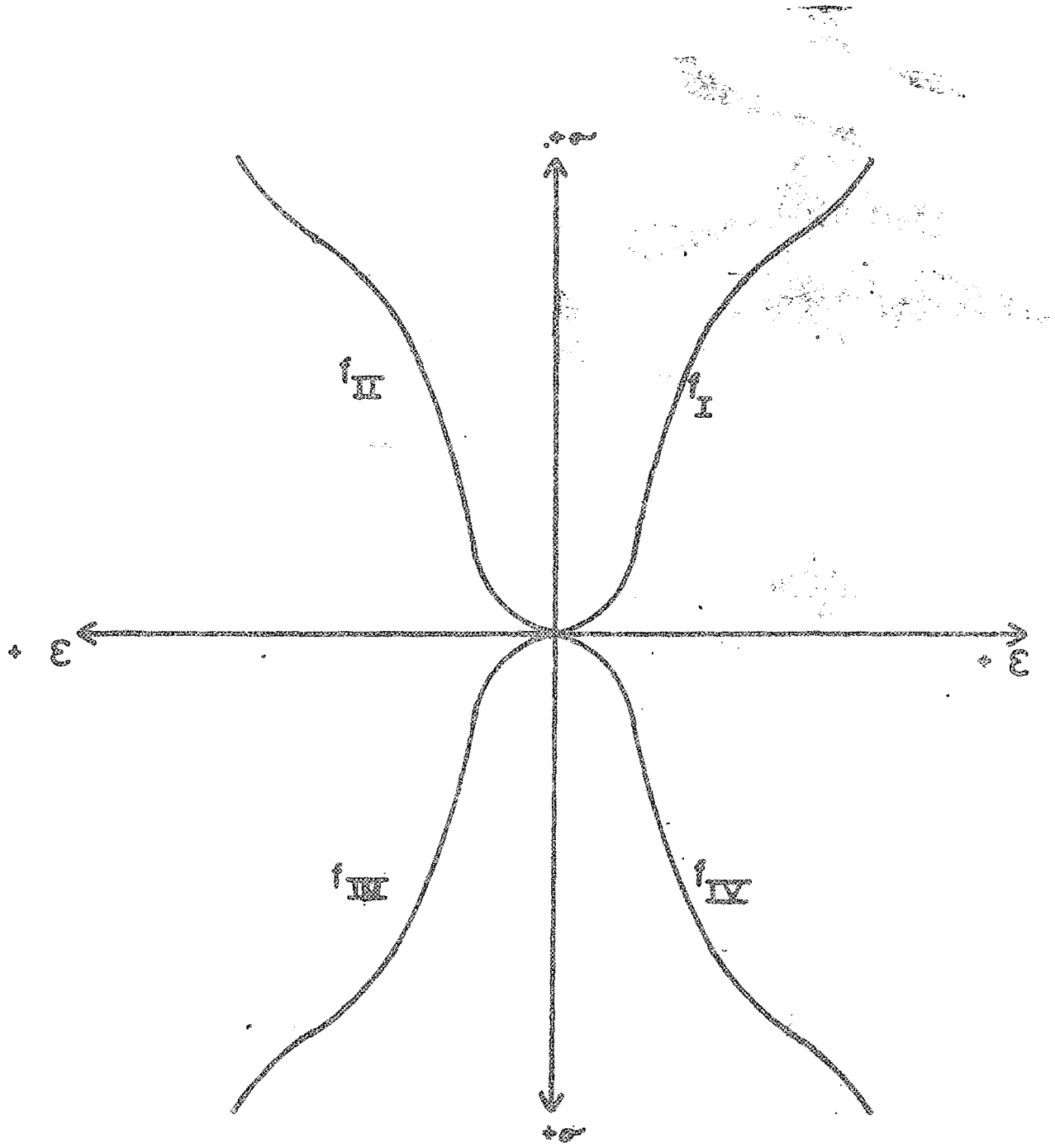

Figure 4

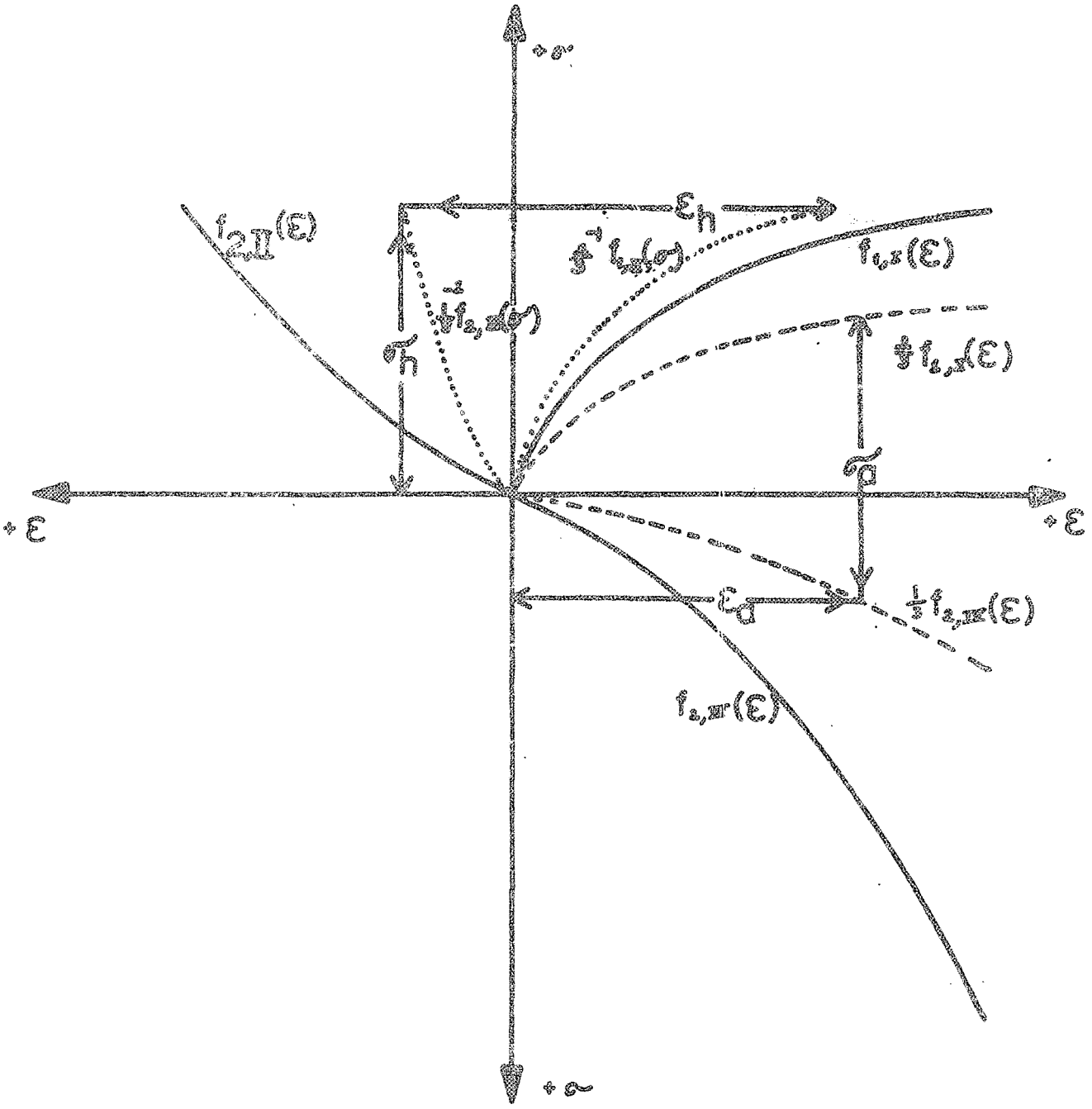
+σ
+ε
+ε
+σ
ε_h
ε_a
σ_h
σ_a
$f_{2II}(\varepsilon)$
$f_{1,x}(\varepsilon)$
$\frac{1}{3}f_{1,x}(\sigma)$
$\frac{1}{3}f_{1,x}(\varepsilon)$
$\frac{1}{3}f_{2,x}(\sigma)$
$\frac{1}{3}f_{2,x}(\varepsilon)$
$f_{2,III}(\varepsilon)$

Figure 5

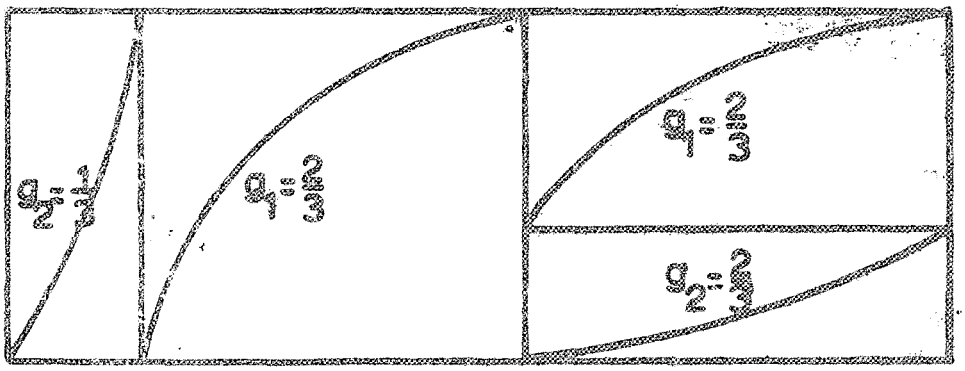

Figure 7

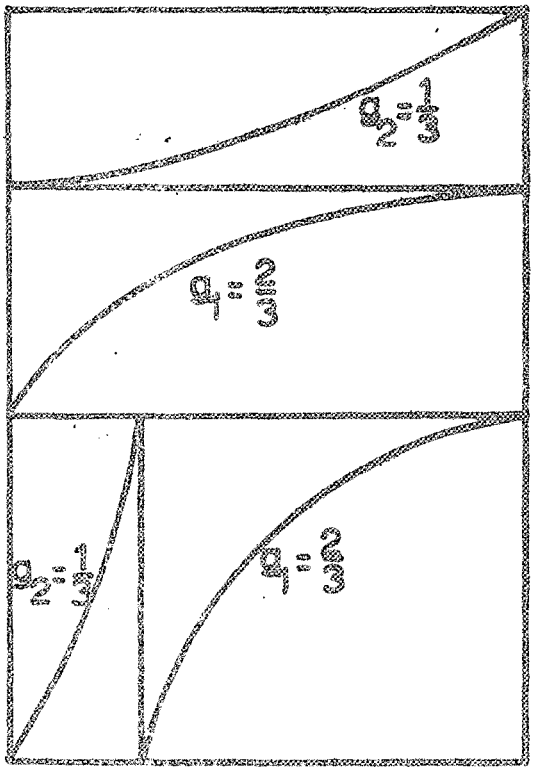

Figure 6

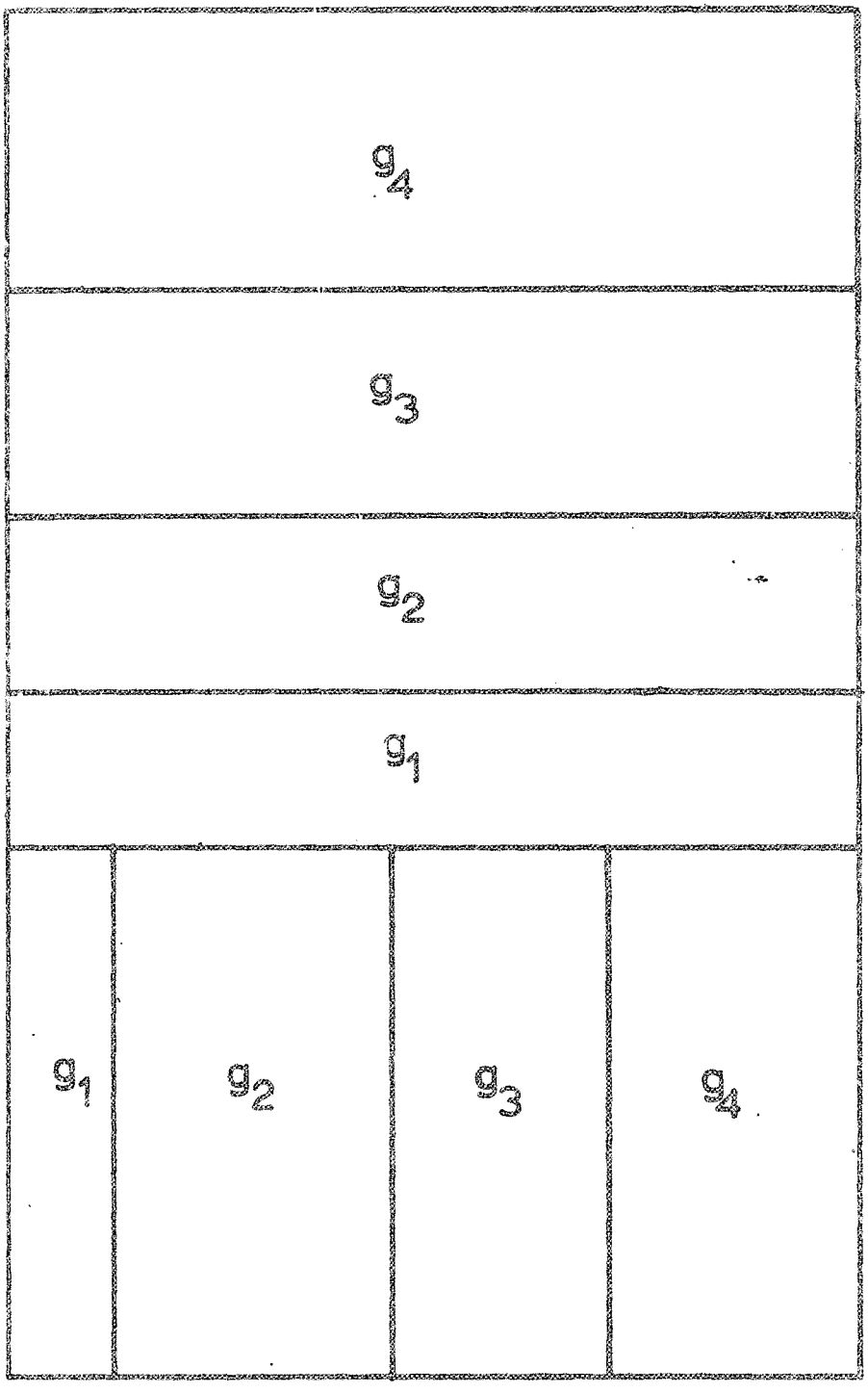

Figure 8

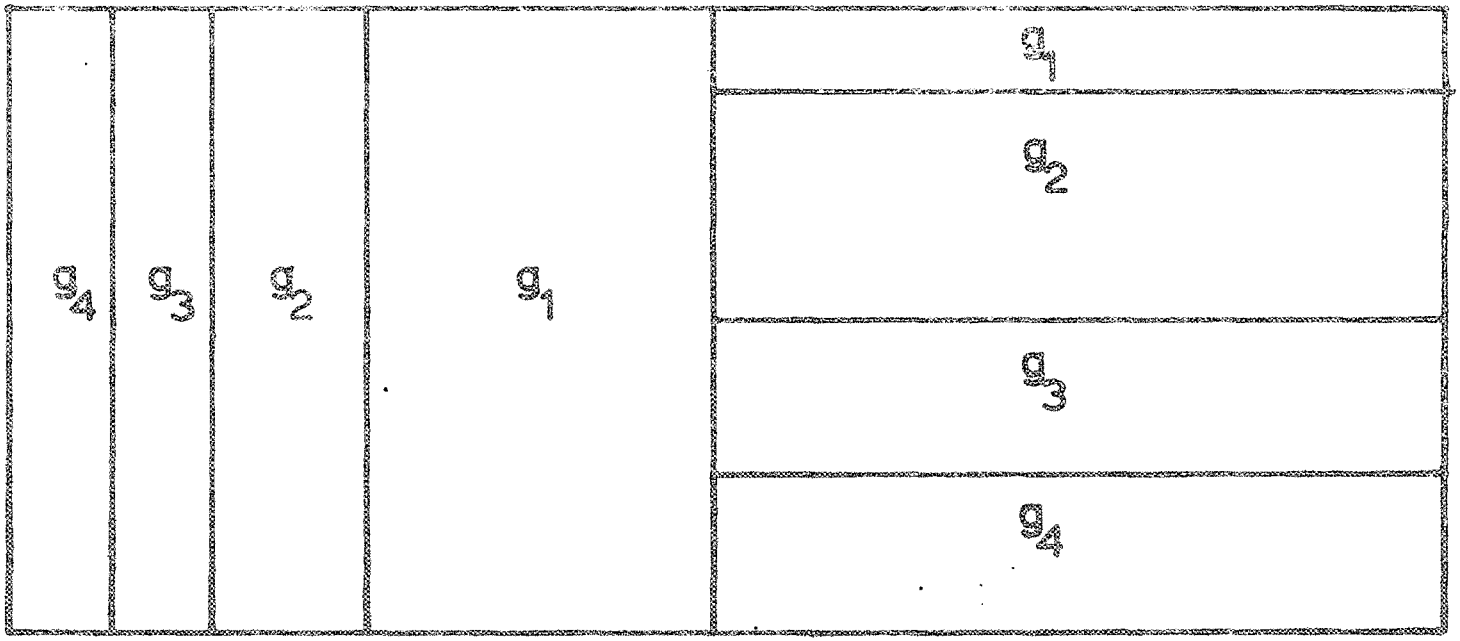

Figure 9

A GRAPHICAL APPROACH TO DETERMINE THE ELASTIC DEFORMATION OF LINEAR N-PHASE COMPOSITE SOLIDS

by

Michael R. A. Erdey, Professor

Electrical Engineering Department
School of Engineering
Tuskegee Institute,
Alabama 36088

ABSTRACT

This paper presents a graphical approach for the determination of the deformability of n-phase, linear, composite solid materials. Throughout the paper, the laminated model approximation is used. In this approximation, the "arithmetic-mean" model provides an upper limit for the modulus of elasticity of the composite material, while the "harmonic-mean" model provides a lower limit. Their combination gives a still better approximation for "composite hard" and "composite soft" materials.

INTRODUCTION

In a recent paper (6), the model approach to two-phase composite solids was discussed with the aid of various models. In this article, the author used only the laminated models (4,5,6) generalizing the technique to n-phase linear composite solids.

In the referred papers (4,5,6), only the analysis part of the problem was exposed. In that case, the modulus of elasticity of the composite material is found from the moduli of elasticity of the composite material and their blending proportions.

In the present paper, the synthesis problem is attacked. In this case, the modulus of elasticity of the required composite material is given along with the moduli of elasticity of the component materials. The unknowns are the blending ratios of the component materials that have to be found.

In the synthesis problem for two materials, there is a unique solution, but the formula is quite complicated; but there is no more a unique solution to the problem of the n-phase case and there is much freedom left to the designer to introduce additional constraints on the basis of economical or other basis. In problems where lot of flexibility is left to the designer, graphical techniques are very advantageous, since the best natural optimizer is the human eye.

For all $n \geq 3$ cases, the same graphical technique is used.

The Laminated Models

Laminated models are obtained if we introduce some simplifying assumptions. If the internal structure of a material is such that the strain is the same over any section of the composite material, while the stresses in the phases are proportional to the moduli of elasticity of the phases, we can represent the composite material with the laminated model of Fig. 1. In this case,

$$E_a = g_1 E_1 + g_2 E_2 + \text{----} + g_k E_k + \text{----} + g_n E_n \quad (1)$$

where

E_a = modulus of elasticity of the composite material,

E_k = modulus of elasticity of the k-th phase

g_k = fractional volume of particles (percent/100)

This model will be referred to from now on as the "arithmetic mean" model, since E_a is obtained by weighted arithmetic mean. The subscript a referes to this fact, too.

Another simple model is obtained if it is assumed that the stress is the same over any section of the composite material, while the deformations of the phases are inversely proportional to the moduli of elasticity of the phases. This case can be represented with the laminated model of Fig. 2 and described by equation (2).

$$\frac{1}{E_h} = \frac{g_1}{E_1} + \frac{g_2}{E_2} + \text{----} + \frac{g_k}{E_k} + \text{----} + \frac{g_n}{E_n} \quad (2)$$

This model will be referred to from now on as the "harmonic mean" model reminding us that E_h is obtained as a harmonic mean. The h subscript refers to the same fact.

In both cases, the following interrelation holds:

$$g_1 + g_2 + g_3 + \text{----} + g_n = 1 \qquad (3)$$

Both models can be represented with their electrical equivalents. E_k can be replaced by the R_k resistance of a rheostat and the g_k blending ratio can be represented by the length proportion between the sliding arms of the pertinent rheostat. In this analog, equation, (1) can be represented with the series connected rheostat sections of Fig. 3-a. Instead of rheostats, we could represent equation (1) with the series connected resistors of Fig. 3-b. Similar equation (2) can be represented with the parallel connected resistors of Fig. 4. Instead of rheostats or resistors, we could have chosen variable inductors or fixed inductors with the same interconnection pattern.

The reader is reminded that, to the parallel laminations of Fig. 1 in the electrical analog of Fig. 3-b a series interconnection corresponds. In a similar way , the electric analog of the series laminations of Fig. 2 are the parallel connected resistors of Fig. 4. This is the consequence of the inverse analogy that we have used. If we had replaced E_k with a G_k conductance, direct analog would have been obtained showing up the same type of patterns between the laminations and the interconnection pattern of the pertinent conductances.

Instead of electrical network analogs, mechanical analogs could have been chosen with series or parallel connected springs to represent the laminated model.

Popovics pointed it out (6) that E_a represents an upper bound for the modulus of elasticity of the composite material, while E_h gives a lower bound for the modulus of elasticity. A better approximation is obtained if E_a and E_h are further combined.

$$E_A = \frac{E_a + E_h}{2} \tag{4}$$

Equation (4) will be a better approximation when there is a continuous phase with one of the higher E materials, while the other phases are dispersed in it. On the other hand, if the continuous phase has one of the lower E values, then we get a better approximation in the form of equation (5).

$$\frac{1}{E_H} = \frac{0.5}{E_a} + \frac{0.5}{E_h} \tag{5}$$

Therefore, equation (4) will be referred to from now on as the "composite hard" model and equation (5) as the "composite soft" model.

The laminated models of the "composite hard" and "composite soft" models can be found in Fig. 5-a and b while their resistive network models are given in Fig. 6-a and b.

In order to handle the problem in a convenient graphical form, equation one is rewritten in the form of equation (6)

$$E_a = E_n + (g_1 + g_2 + \ldots + g_{n-1})(E_{n-1} - E_n) + (g_1 + g_2 + \ldots + g_{n-2})(E_{n-2} - E_{n-1}) + \ldots + g_1(E_1 - E_2)$$

assuming that subscripts were chosen in such a way that $E_1 > E_2 > \ldots > E_{n-1} > E_n$ relation is satisfied.

In the following substitutions are made in equation (2)

$$\frac{g_1}{E_1} = \frac{\chi_2}{E_2}, \quad \frac{g_2 + \chi_2}{E_2} = \frac{\chi_3}{E_3}, \cdots \frac{g_{n-2} + \chi_{n-2}}{E_{n-2}} = \frac{\chi_{n-1}}{E_{n-1}}, \frac{g_{n-1} + \chi_{n-1}}{E_{n-1}} = \frac{\chi_n}{E_n}$$

then we obtain equation (7)

$$\frac{1}{E_h} = \frac{g_n + \chi_n}{E_n}$$

In the particular case of n = 4 equation (6) and (7) and the substitutions are the following:

$$E_a = E_4 + (g_1 + g_2 + g_3)(E_3 - E_4) + (g_1 + g_2)(E_2 - E_3) + g_1 (E_1 - E_2) \quad (8)$$

$$\frac{g_1}{E_1} = \frac{\chi_2}{E_2}, \frac{g_2 + \chi_2}{E_2} = \frac{\chi_3}{E_3}, \frac{g_3 + \chi_3}{E_3} = \frac{\chi_4}{E_4}$$

$$\frac{1}{E_h} = \frac{g_4 + \chi_4}{E_4} \quad (9)$$

These interrelations for a particular E_1, E_2, E_3, E_4 set are graphically given in Fig. 7. Note that the magnitudes of all E's are between 0 and 1 which we are allowed to do if we factor out the same power of 10 everywhere and will take into account at the end of the procedure.

The constructions in Fig. 7 are basically very simple. Point 0 is interconnected on the right with E_1, E_2, E_3 and E_4. At the left E_1 is interconnected with Q_1 (end of g_1 interval). The intersection of $\overline{E_1 Q_1}$ with the horizontal line at E_2 level gives Q_4. Similarly, $\overline{Q_4 Q_2}$ (where Q_2 is at the end of the g_2 interval) intersects the E_3 level at Q_5. Repeating the process with $\overline{Q_5 Q_3}$ we obtain Q_6. Dropping vertical lines from Q_4, Q_5 and Q_6 to the base and notating their intersections with the base and the horizontal lines at E_3 and E_4 levels we obtain Q_7, Q_8, Q_9, Q_{10} and Q_{11} points. And thus, we have the basic framework for the graphical evaluation of E_a and E_h.

Let's generate first E_a. Since the E_4 height is already given we have to generate $(g_1 + g_2 + g_3)(E_3 - E_4)$, but this is equal to $\overline{P_8 P_9} = \overline{P_{11} E_4}$. Similarly, $(g_1 + g_2)(E_2 - E_3)$ is equal to $\overline{P_4 P_5} = \overline{P_{10} P_{11}}$ and finally $g_1(E_1-E_2)$ is equal to $\overline{P_1 P_2} = \overline{E_a P_{10}}$. And thus,

$$E_a = E_4 + \overline{P_{11} E_4} + \overline{P_{10} P_{11}} + \overline{E_a P_{10}} \qquad (10)$$

The reader can see that E_a could be obtained if we draw from point P_1 (the point obtained by the intersection of the vertical line drawn from Q_1 with $\overline{OE_1}$) a parallel line to $\overline{O E_2}$. Where this line intersects the vertical drawn from Q_2 we obtain P_2. From P_2 we draw parallel to $\overline{O E_3}$ which will intersect the vertical from Q_3 at P_6. Finally, the parallel line drawn from P_6 to $\overline{O E_4}$ intersects the right boundary at E_a.

The substitution interrelations can be obtained from similar triangles as follows

$$\frac{g_1}{E_1} = \frac{X_2}{E_2} \quad \text{from} \quad O Q_1 E_1 \Delta \sim Q_7 Q_1 Q_4$$

$$\frac{g_2 + X_2}{E_2} = \frac{X_3}{E_3} \quad \text{from} \quad Q_7 Q_2 Q_4 \Delta \sim Q_8 Q_2 Q_5 \Delta$$

$$\frac{g_3 + X_3}{E_3} = \frac{X_4}{E_4} \quad \text{from} \quad Q_8 Q_3 Q_5 \Delta \sim Q_{11} Q_6 Q_5 \Delta$$

Drawing through points 1 and Q_6 a line at the intersection with the left boundary gives E_h, which can be verified from equation (9), again with a pair of similar triangles

since $\frac{1}{E_h} = \frac{g_4 + X_4}{E_4}$ can be seen from $O 1 E_h \Delta \sim Q_9 1 Q_6 \Delta$

Now that we have both E_a and E_h, we can find E_A and E_H. Since E_a is just the arithmetic mean of E_a and E_h on the right boundary, we just halved $\overline{E_a E_h}$. E_H is found with the harmonic mean process with the two dotted lines. The previous Q_6 point was this time replaced by point R.

In the general n-phase case of equations (6) and (7), the process is exactly the same. The E_1 to E_n points on the right are interconnected with point O. On the left, similar to the four E_1, Q_4, Q_5, Q_6 points with a similar process a set of n points are generated on the levels of the pertinent E_1 - E_n points. When E_a and E_h are obtained, E_A and E_H are obtained with exactly the same process that we have seen in Fig. 7.

The technique was demonstrated in the case of the analysis problem, to familiarize the reader with it. Since in the case of analysis, the combinations of arithmetic and harmonic means are only involved, there is no need to introduce graphical techniques. On the other hand, the synthesis problem as we will see in the next section will become quite complex analytically and it is worth to introduce graphical techniques.

The Synthesis Problem

In the synthesis problem, we assume that E_1, E_2 ... E_n and in addition either E_A or E_H is given, depending upon wether we assume a composite hard or composite soft case, and the problem is to find the g_1, g_2 ... g_n blending ratios.

In case of only two components, the solution is unique. If composite hard model is assumed, equation (11) gives the solution for g_1 while the composite soft case is given by equation (12).

$$g_{1A} = \frac{2E_A + E_1 - E_2 \pm \sqrt{(2E_H + E_1 - E_2)^2 + 8E_1(E_2 - E_A)}}{2(E_1 - E_2)} \quad (11)$$

$$g_{1H} = \frac{E_H(E_1 - E_2) - 2E_1E_2 \pm \sqrt{[E_H(E_1 - E_2) - 2E_1E_2]^2 + 8E_1E_2E_H(E_H - E_2)}}{2E_H(E_1 - E_2)} \quad (12)$$

The uniqueness is not satisfied anymore for the n 2 cases. For these cases, an additional n-2 parameters can be varied within reasonable limits, and this is exactly the case where the graphical approach will be helpful.

Lets assume that we have a 3-phase problem where E_1, E_2, E_3 and E_A are given, a particular set of these values are given in Fig. 8. In addition, one parameter can be chosen freely within allowable limits. Lets say that we want to choose freely g_1. We can see that the smallest value of g_1 is obtained if $E_a = E_A$ and $g_3 = o$. Graphically, this condition is equivalent of drawing a parallel to $\overline{O\,E_2}$ through E_A. This line intersects $\overline{O\,E_1}$ in P_1 from where by dropping a perpendicular to the base we obtain the min value of g_1. The intersection of $\overline{E_n I}$ with the E_3 level will be further to the right if E_n is larger. The maximum value of $E_n = E_A$. In this case, the intersection point is point P_2. Since this

point is always to the right of the right end of the pertinent g_1 interval $\overline{O\ Q_2}$ gives only an upper bound to g_1. Since for any g_1 the maximum value of E_a is obtained by letting $g_3 = 0$, the parallel line to $\overline{O\ E_2}$ through point P_3 defines the upper bound for E_a.

The conditions on Fig. 8 were given in such a way that the allowable range for either g_1 or E_a was quite small. In Fig. 9 we have a case for a 3-phase problem where the allowable range for both g_1 and E_a is larger. Since it is quite obvious that larger proportions from the higher values of E's will increase the value of E_a and since it is well known that the human eye is the best optimizer if graphical di plays are available, after a little practice, the designer can easily choose the most desirable solution at a glance.

In Fig. 9, E_A is chosen almost equal to E_2. This is done to stress again how much we can see right away the solution at the beginning if we approach it from the heuristicpoint of view. Therefore, E_1 and E_3 will almost serve to compensate each other. If we take larger proportion of them, a smaller proportion of E_2 will remain. A larger proportion E_1 will mean a larger E_a. Thus, we see the intricate interrelations of these quantities inaa heuristic manner.

Let's assume that we have decided to use E_a as shown in Fig. 9. Thus, we have up to now, the 3 boundary lines with E_1, E_2, E_3, E_4 and E_a points on the diagram. Since E_h is in a symmetric position to E_a relative to E_A this is our next point on the diagram. Afterwards, we can interconnect point O with E_1, E_2 and E_3. Then we can draw a parallel to $\overline{O\ E_3}$ through E_a which intersects O E_1 at point P_4.

Since we don't know yet where the parallel line $\overline{O\ E_2}$ will intersect $\overline{P_4\ E_a}$ and $\overline{O\ E_1}$, therefore tentatively we take the longest one through E_a which intersects $\overline{O\ E_1}$ at P_1. A vertical line dropped to the base from P_1 gives P_2. If E_h on the left is interconnected with point 1 at the right corner and extended until it intersects the E_2 level we obtain point P_3. According to the basic patterns that were demonstrated in Fig. 7. one of the major construction lines has to go through points P_2 and P_3. The other extreme case is the one when the parallel to $\overline{O\ E_2}$ shrinks into point P_4, the base projection of which is P_5. According to our basic pattern, the line defining the boundary point between g_1 and g_2 goes through P_5 and P (the intersection point of $\overline{E_h 1}$ with the E_3 level). Where the extensions of $\overline{P_2 P_3}$ /intersect each other, we obtain point P_6. All lines go through P_6 which cut out the left end of the g_2 interval from the base line as the parallel lines to $\overline{O\ E_2}$ are changed. In the case of the solution this line has to go through point E_1 too, thus all we have to do is to interconnect P_6 with E_1 to obtain at their intersection point the P_7 solution. Thus, $g_1 = \overline{O\ P_7}$. The intersection of $\overline{P_7 E_1}$ with the E_2 level yields point P_{11}. Where the extension of $\overline{P_{11} P}$ intersects the base, we obtain P_{10} the right end point of the g_2 interval. Thus, $g_2 = \overline{P_7 P_{10}}$ and $g_3 = \overline{P_{10} 1}$. We could have obtained g_2 by intersecting $\overline{O\ E_1}$ at point P_8 with the vertical line drawn from the base at P_7. The parallel to $\overline{O\ E_2}$ from P_8 intersects $\overline{P_4\ E_a}$ at P_3. The vertical line drawn from P_9 has to intersect the base at the obtained P_{10} point, thus, the second approach can be used as a check to the accuracy of the previous construction.

In Fig. 10, the solution to a four phase problem can be seen In this case, in addition to the given E_1, E_2, E_3, E_4 and E_A values two additional parameters can be freely chosen within the allowable limits. Lets say that we are choosing E_a and $g_1 = \overline{O\,P_1}$ with values that can be seen in Fig. 10; in this case, after all these points are put on the three sides of the framework point O is interconnected with E_1, E_2, E_3, E_4 and point E_1 with P_1. Next, we drop a vertical line to the base at P_1 which intersects $\overline{O\,E_1}$ at P_2. The parallel to $\overline{O\,E_2}$ from P_2 intersects the parallel to $\overline{O\,E_4}$ from E_a at P_3. Similar to the previous case, we don't know the exact intersection points of the parallel to $\overline{O\,E_3}$ with $\overline{P_2P_3}$ and $\overline{P_3E_a}$, therefore, we will choose again the two extreme cases in between where the actual solution has to lay. The parallel through E_a intersects $\overline{P_2P_3}$ at P_4. The projection of P_4 at the base is P_5. Through the P_6 point where the $\overline{E_nI}$ line intersects the E_3 level has to go through the line from P_5 which goes through the left end of the g_3 interval under the given assumption. When the parallel interval shrinks into point P_3, then the g_3 interval shrinks into the P_7 point which means that the line crossing the base at its left end is the same as the line crossing the base at itsright end and, therefore, it has to go through point P where $\overline{E_nI}$ intersected the E_4 level. At the intersection of the extensions of $\overline{P_5P_6}$ and $\overline{P_7P}$ is P_8. This is the common intersection point of all those lines which intersect the base at the left end of the g_3 interval as the parallel lines to $\overline{O\,E_3}$ are shifted. For the solution, this line has to go through point P_9 (intersection of $\overline{E_1P_1}$ with the E_2 level)

also, the solution is obtained by extending $\overline{P_8P_9}$ until it interacts the base at P_{10}. Thus, $g_2 = \overline{P_1P_{10}}$. At the intersection of $\overline{P_9P_{10}}$ with the E_3 level is P_{11}. The extension of $\overline{P_{11}P}$ intersects the base at P_{12} which is the right end of the g_3 interval. That is, $g_3 = \overline{P_{10}P_{12}}$, $g_4 = \overline{P_{12}1}$. And thus, we have the solution with the assigned E_a, g_1 values. From P_{10} on we could have chosen the other alternative through P_{13}, P_{14} to P_{12} as we have seen in the previous case.

In Fig. 9 and Fig. 10, we have seen the basic patterns for the solution of the 3-phase and 4-phase cases. It is quite obvious from them that the same pattern can be repeated irrespectively from the value of n. In the case E_a is chosen as one of the free parameters, we can choose the first (n-3) g parameters also freely. All that we should look for is/where the line parallel to $\overline{0\ E_n}$ through E_a has its intersection with the line/slope of with the E_{n-2} above the $\overline{0,\ 1}$ and that this point is/to the right of point P (the intersection point of $\overline{E_n 1}$ with the E_n level). Due to the very picturesque diagrams, this can be always/intuitively seen by the designer who can always see within approximately what limits can he vary his parameters. That changes in these diagrams as n increases, is the level on which that line segment starts which will define the dividing end points between g_{n-2} and g_{n-1} segments on the base. For the n-3 case, it started from point E_1, for the n-3 case, from the point on level E_2 and any general n case this starting point will be on level E_{n-2}. A second point for this line can be defined always with the method of the two extreme

positions of the parallel to the $\overline{0\ E_{n-1}}$ line segment.

In the two demonstrated examples, we assumed "composite hard" models. If we would assume a "composite soft" model the problem would be equally simple. As we can see from Fig. 7, if E_H is given we can also choose freely an E_a value (assuming that $n \geq 3$). The R intersection point of $\overline{E_H 1}$ with $\overline{E_a\ 0.5}$ gives the level of E_h. Halving $\overline{E_a E_h}$, we obtain an "equivalent" E_A, from where on the problem is the same as before.

Solution with the Aid of a Graphics Terminal of a Computer

The first described technique can be easily adopted to the graphics terminal of a computer. Since all lines are straight, it can be handled all the way with a light pen. On the other hand, programs can be developed where the designer has to type in only the E_1, E_2, ... E_n, E_A, E_a, g_1, g_2 ... g_{n-3} and a diagram appears on the screen. On the basis of the graphical message of this diagram, the designer can type in the updated values of E_a, g_1, g_2, ---- g_{n-3}. In this conversational mode, the operator can not only find a solution, but can find a whole set of solutions from which he can choose the optimum one.

Since this technique was developed as a part of a NASA project in which an AMIRAN graphics terminal is used, this technique will be adapted to this particular terminal.

It is easy to see that the laminar model is adaptable to analog computers, too. In that case, only summing amplifyers are used while the g blending ratios will be set on potentiometers. Instead of manually changing the potentiometer settings in a true hybrid operation they can be automatically changed until solution (or optimal solution) is reached.

Acknowledgement

This work was sponsored by NASA Grant NGR 01-005-004. The author wishes to thank them for their kind permission allowing this material to be published.

References

1. M. R. A. Erdey: "Rectangular Diagrams and Their Applications to Newtork Theorems". Proceedings of the Sixth Midwest Symposium on Circuit-Theory, pp. F-1 to F-17, Madison, Wisconsin (1963).

2. M. R. A. Erdey: "The Misrepresented Duality and the Rectangular Diagrams". Proceedings of the IEEE Region III Convention, pp. 9.5.1 - 9.5.10, New Orleans, Louisiana (1968).

3. M. R. A. Erdey: "Rectangular Diagrams in Graph Theory". Proceedings of the Eleventh Midwest Symposium on Circuit Theory, pp. 441-456, Notre Dame, Indiana (1968).

4. J. C. Hansen: "Theories of Multi-phase Materials Applied to Concrete, Cement Mortar and Cement Paste". Proceedings of the International Conference on the Structure of Concrete, London, September, 1965.

5. B. Paul: "Prediction of Elastic Constants of Multi-phase Materials". Transactions of the Metallurgical Society of ASME, Vol. 218, pp. 36-41, February, 1960.

6. Popovics, S.: "The Model Approach to Two-phase Composite Solids".

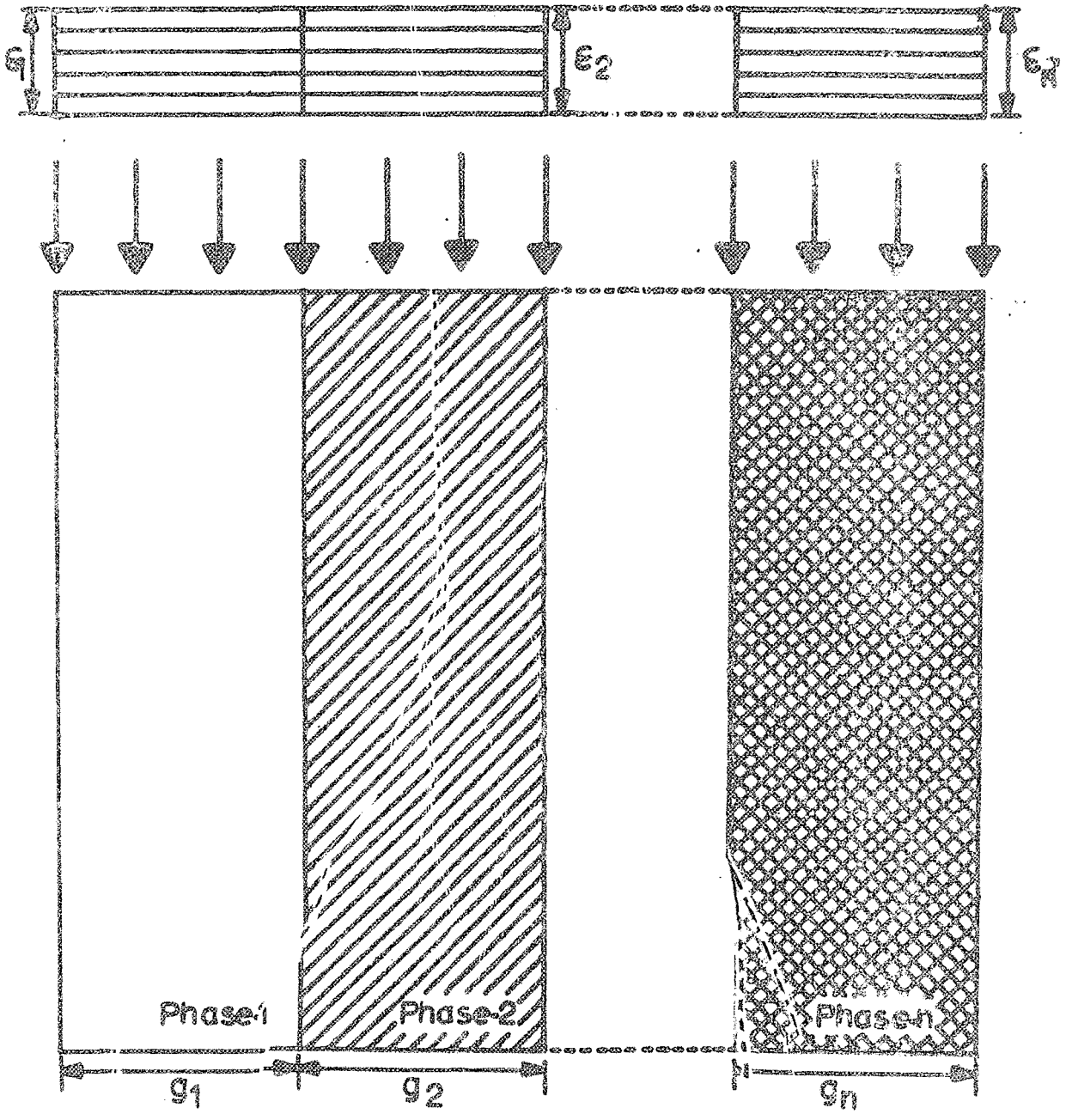

Figure.1

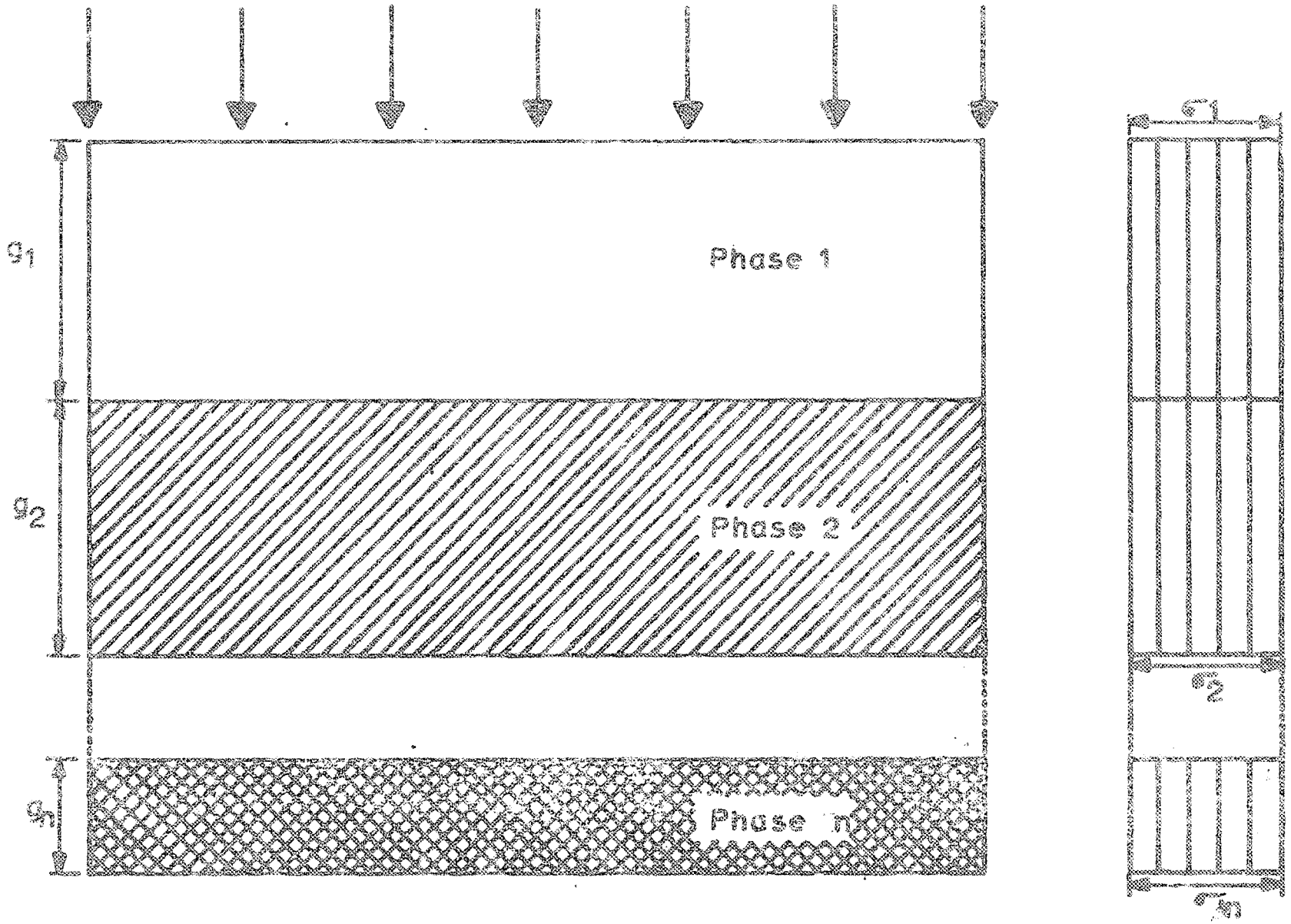

Figure · 2

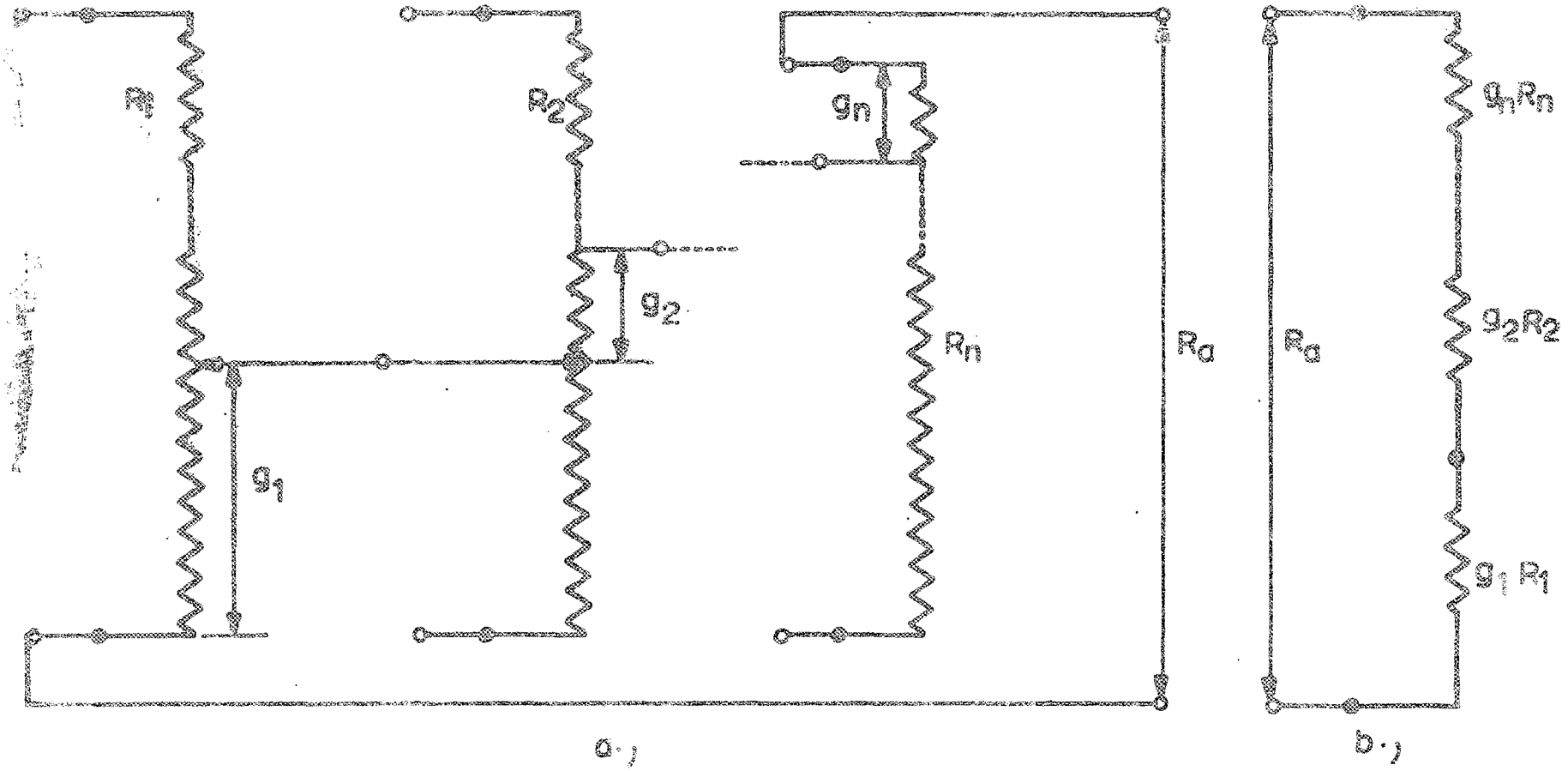

Figure 3

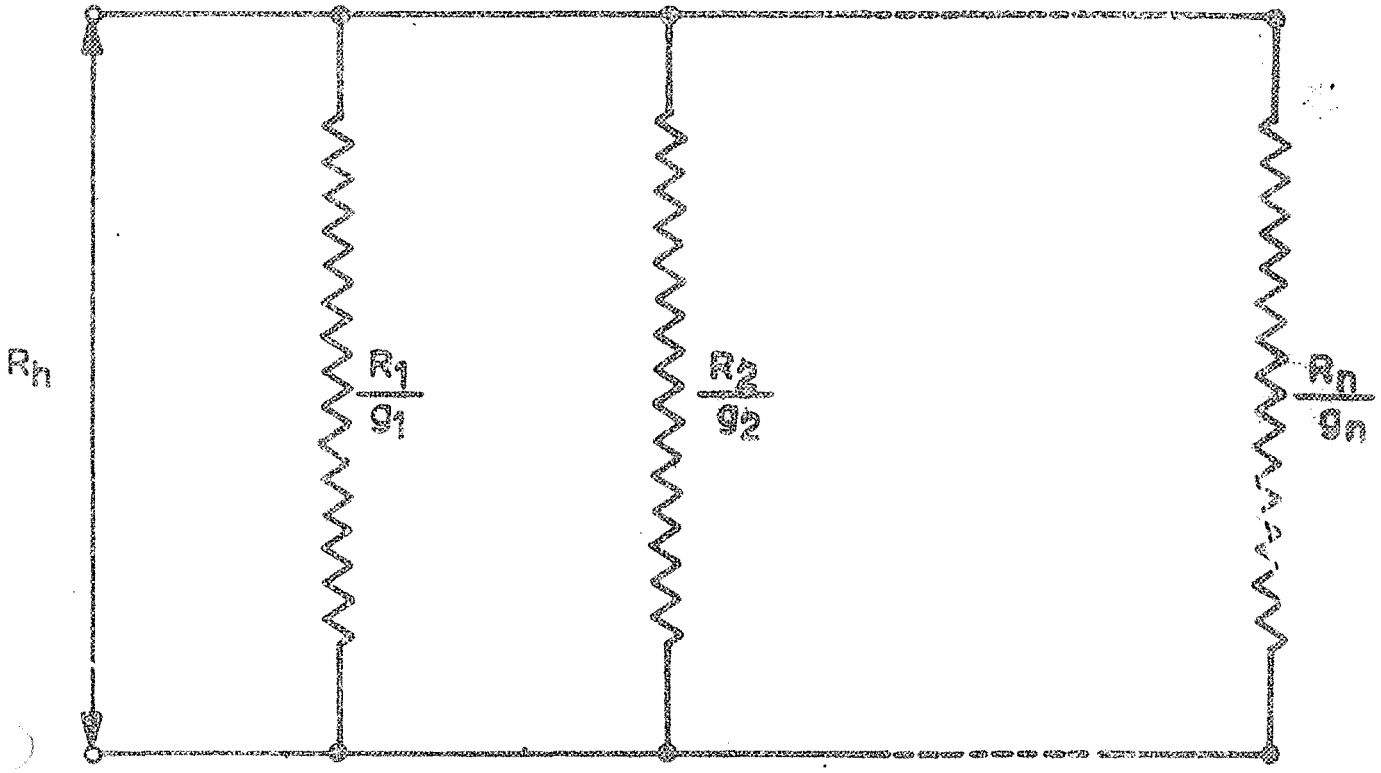

Figure . 4

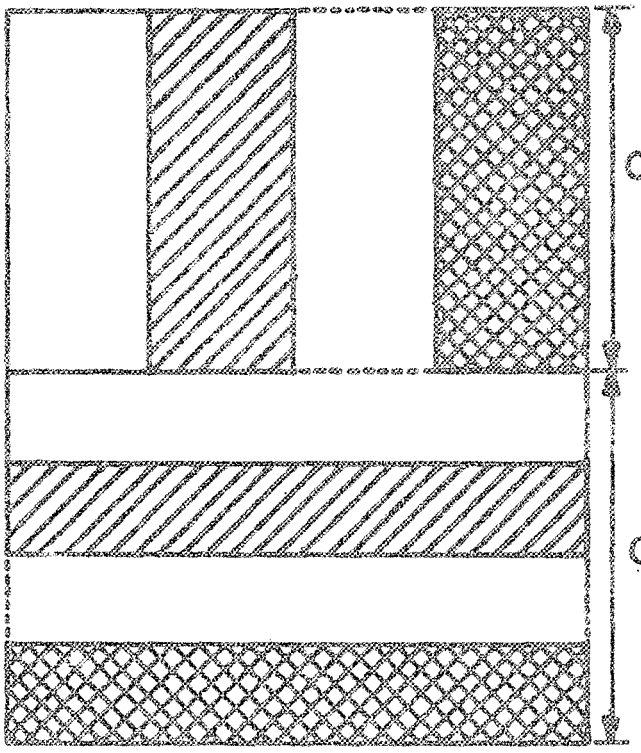

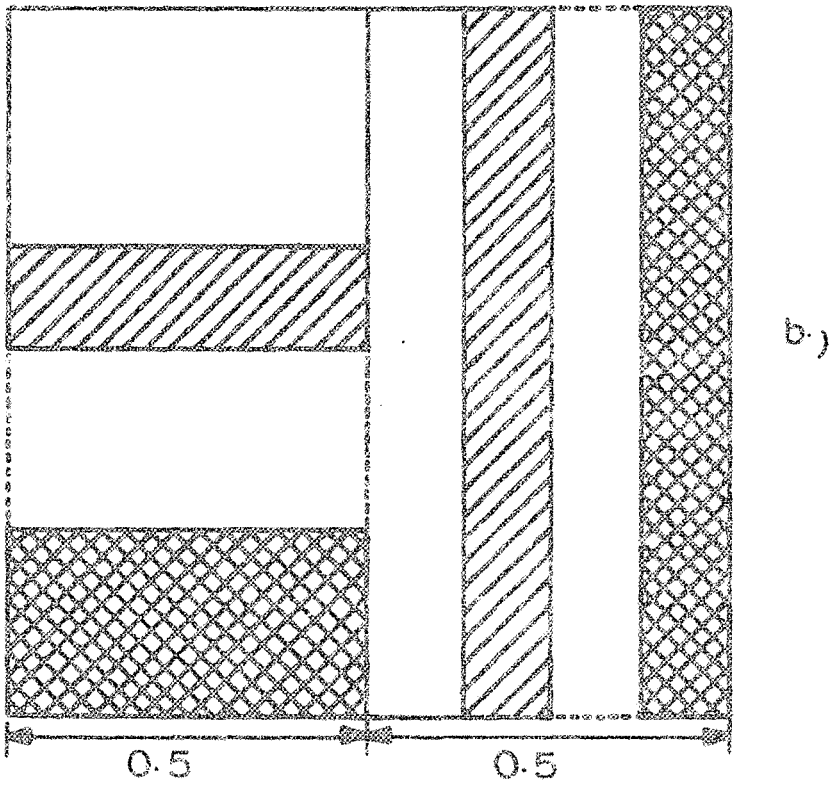

Figure·5

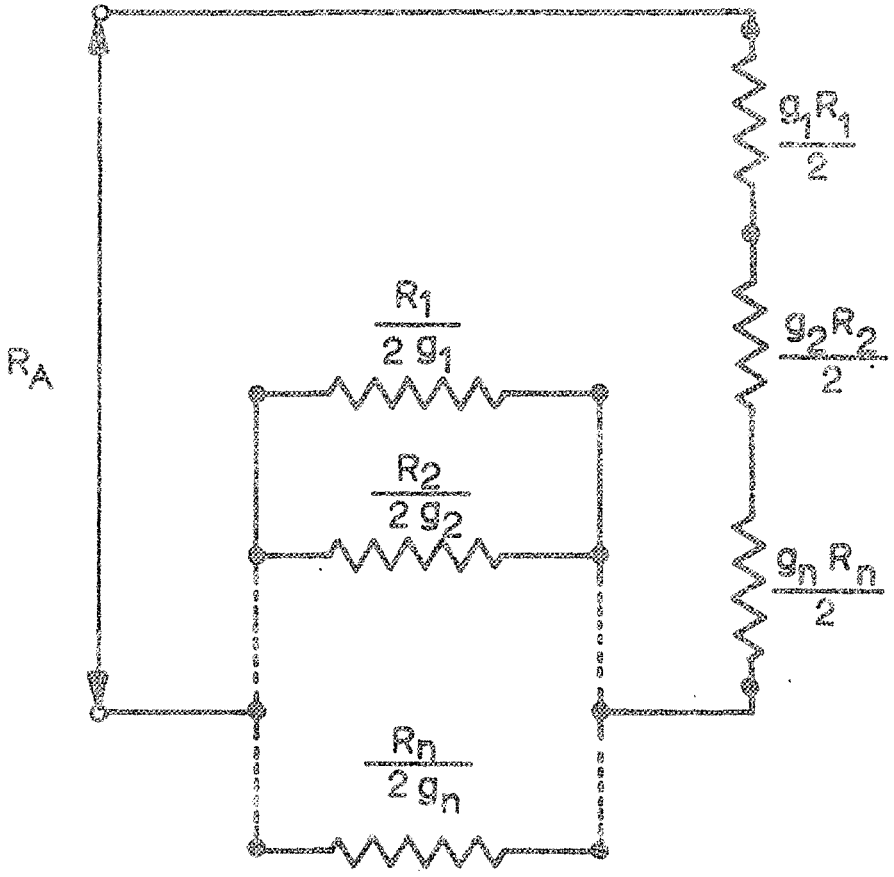
R_A
$\frac{R_1}{2g_1}$
$\frac{R_2}{2g_2}$
$\frac{R_n}{2g_n}$
$\frac{g_1R_1}{2}$
$\frac{g_2R_2}{2}$
$\frac{g_nR_n}{2}$

a.)

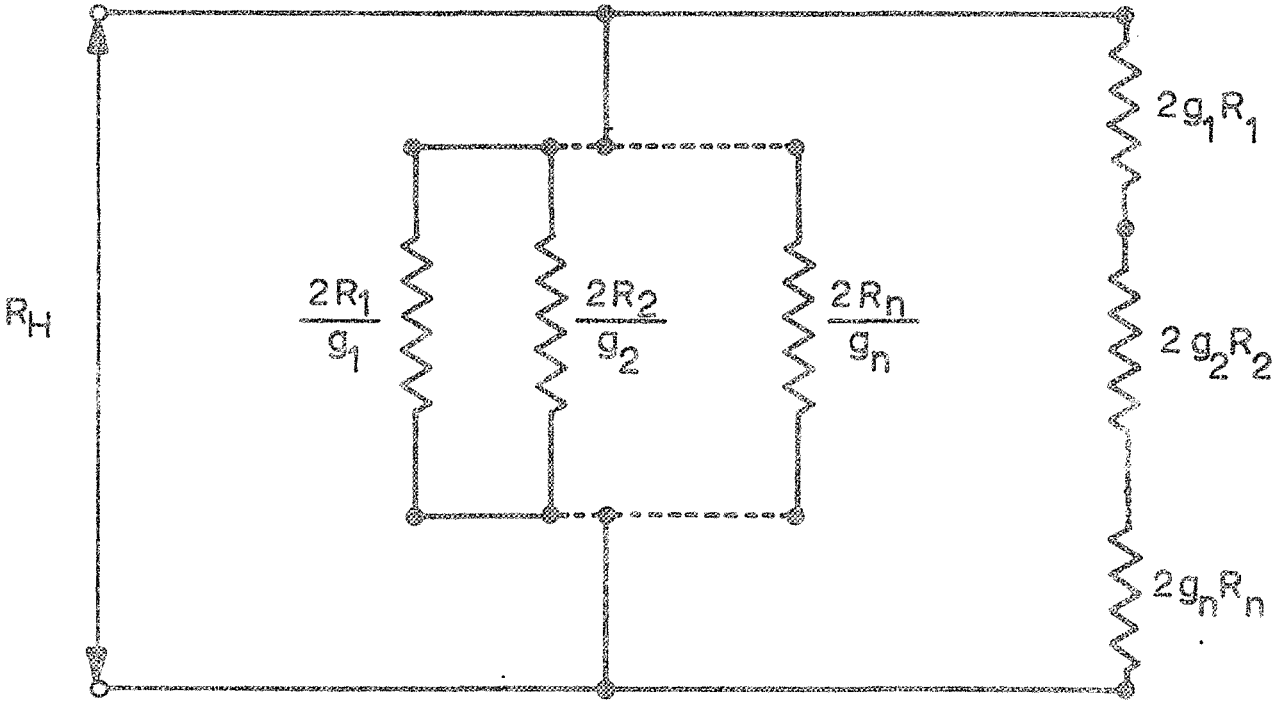
R_H
$\frac{2R_1}{g_1}$
$\frac{2R_2}{g_2}$
$\frac{2R_n}{g_n}$
$2g_1R_1$
$2g_2R_2$
$2g_nR_n$

Figure · 6

b.)

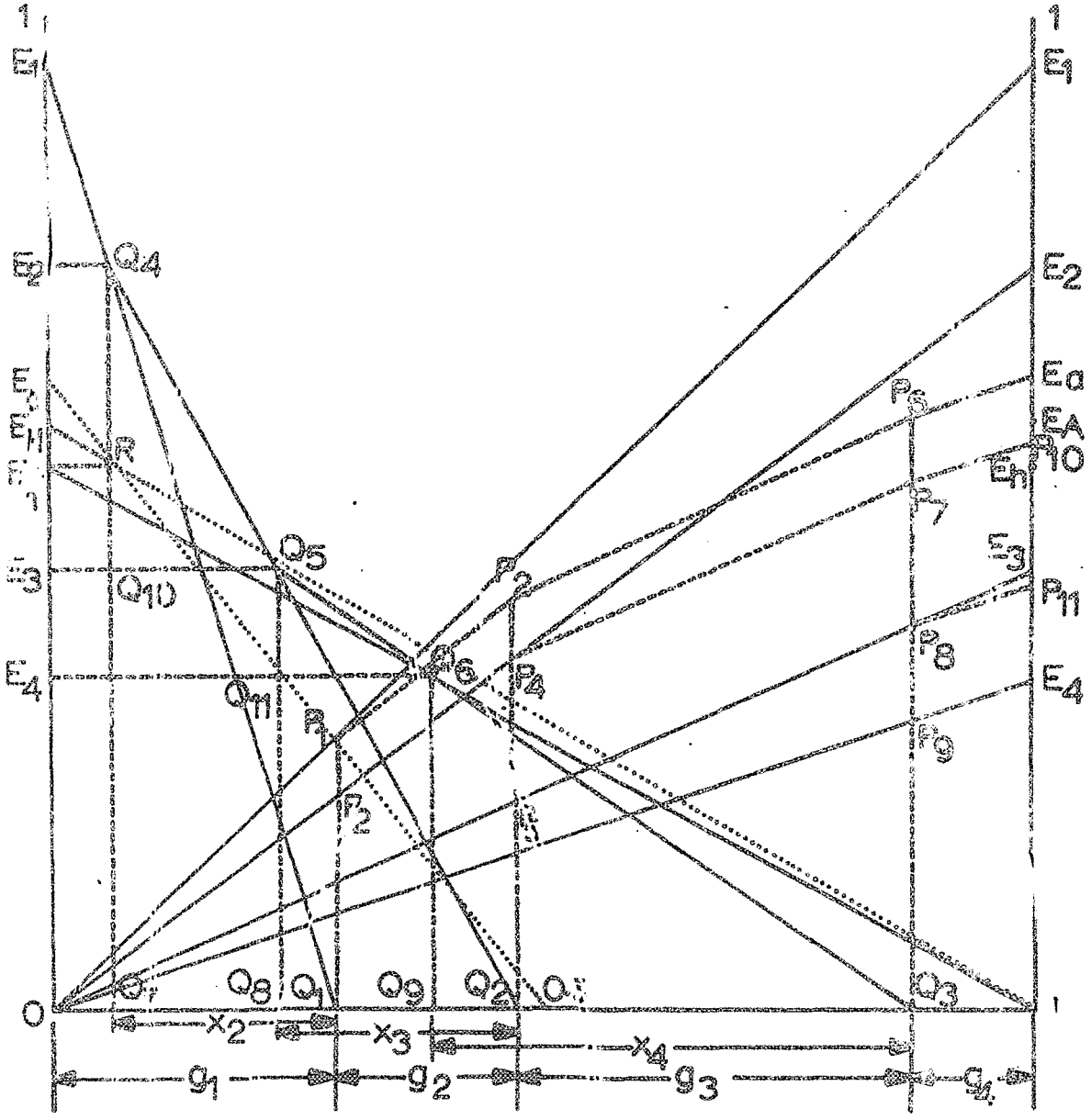
1
E1
E2
E3
E4
Q4
R
Q5
Q10
Q11
P1
P2
P6
P4
P5
P7
P8
P9
P11
E5
E6
E7
E8
E9
E10
E11
Q8
Q1
Q9
Q2
Q3
0
x2
x3
x4
g1
g2
g3
g4

Figure·7

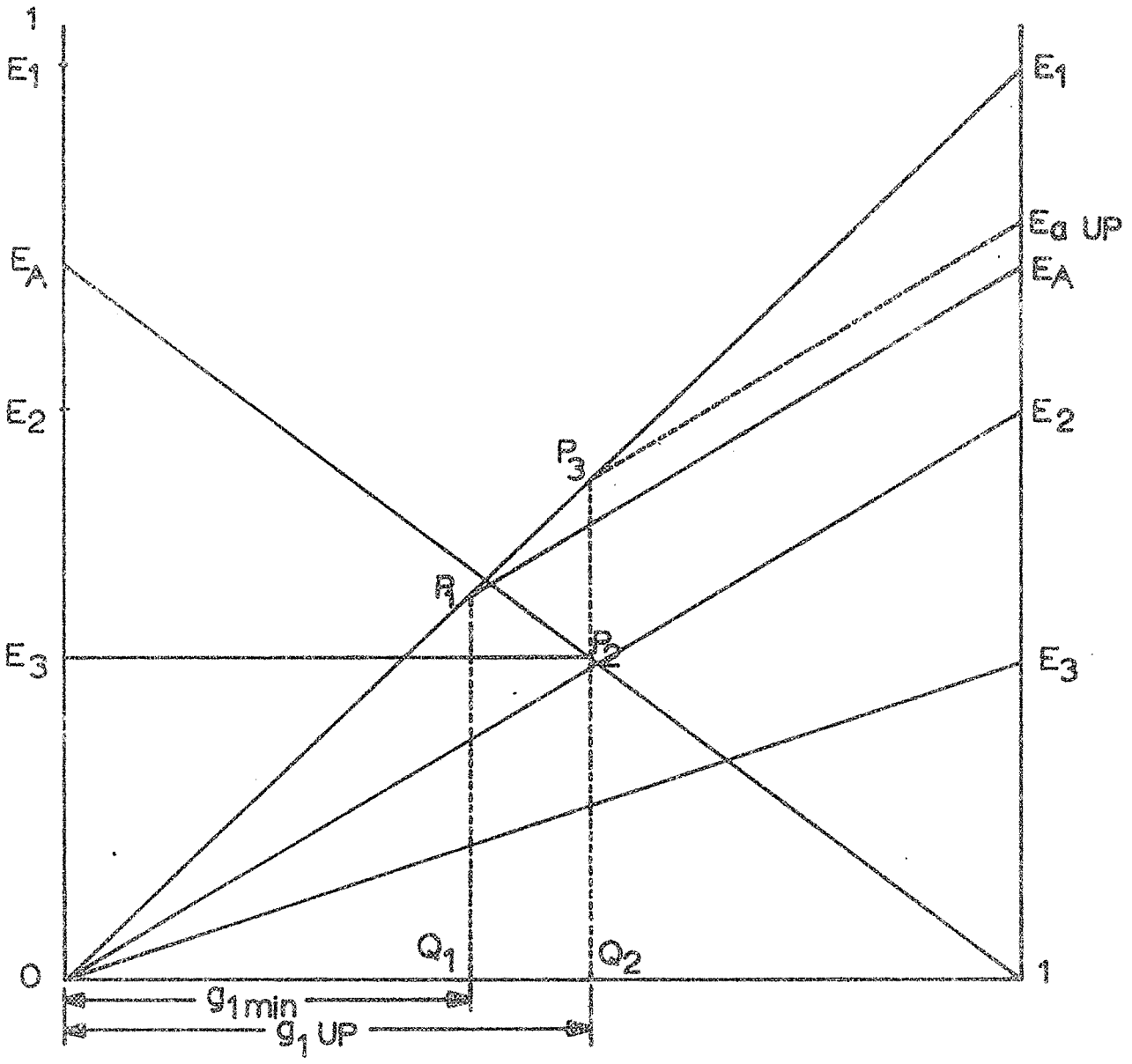

Figure. 8

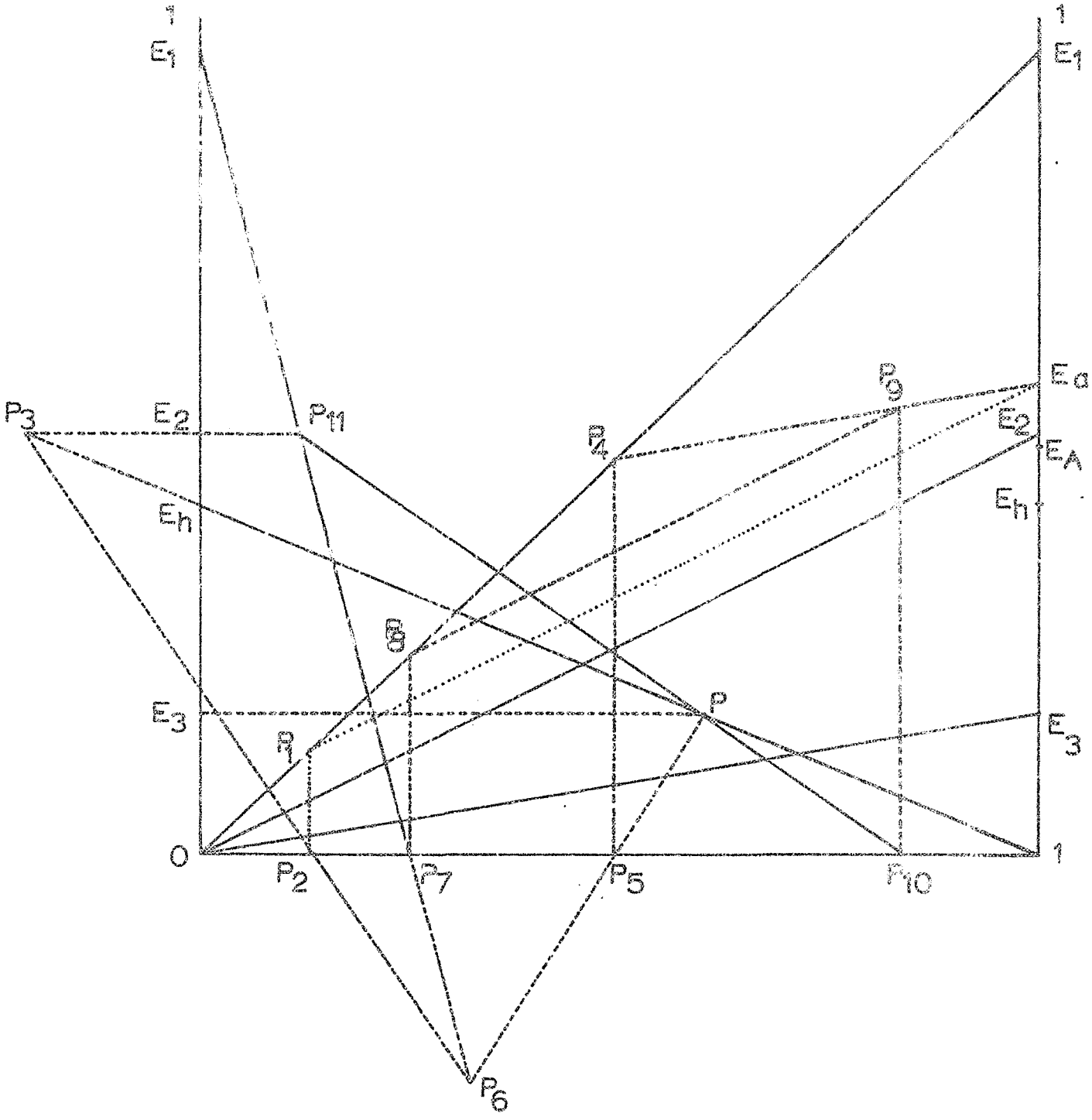

Figure. 9

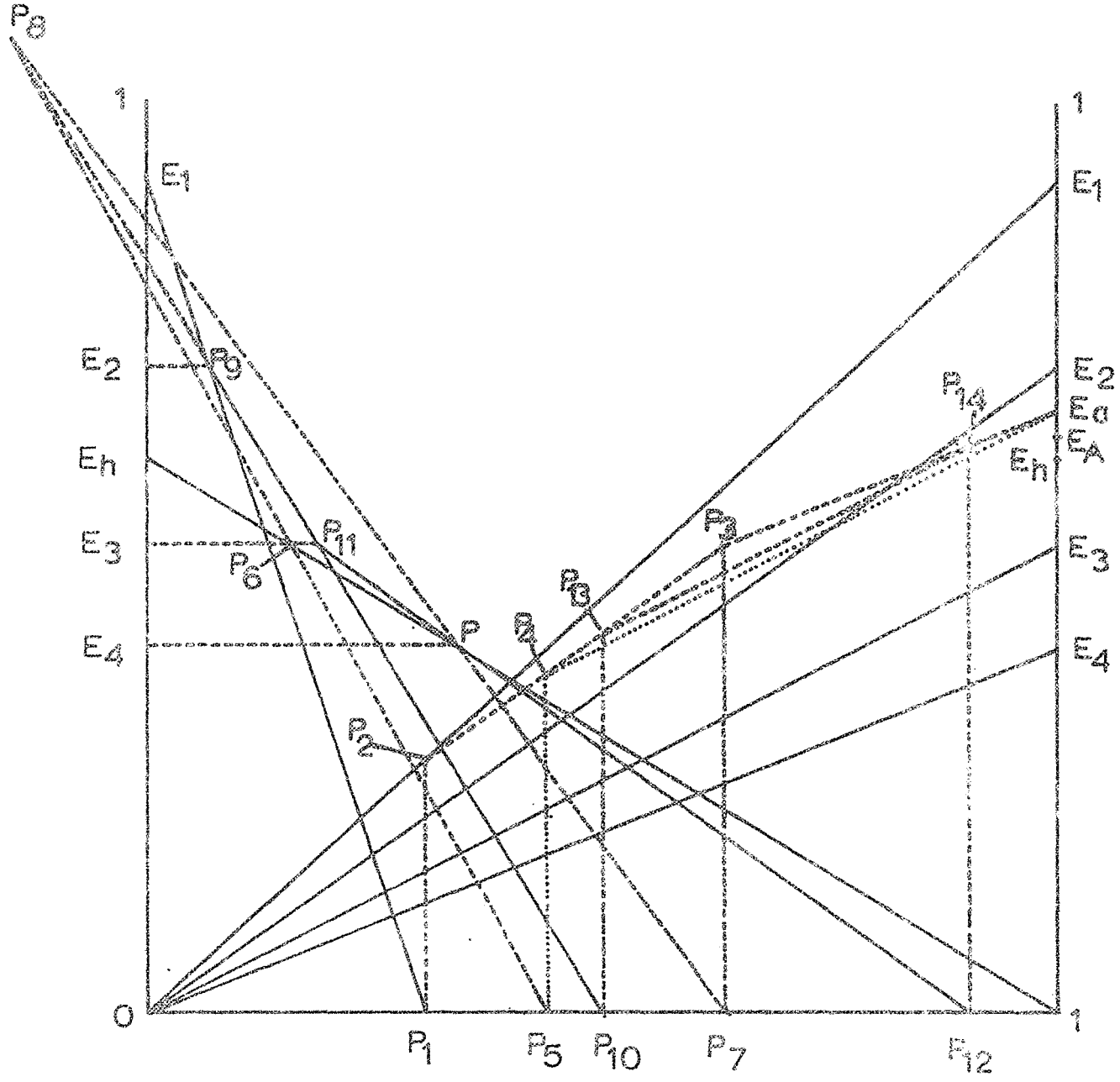
P8
1
E1
E2
P9
Eh
E3
P11
P6
E4
P
P4
P13
P3
P2
O
P1
P5
P10
P7
P12
P14
Ec
EA
1

Figure·10